UC Irvine
UC Irvine Electronic Theses and Dissertations

Title
Microfabricated Platform for the Study of Tunneling Nanotubes

Permalink
https://escholarship.org/uc/item/63k9k3x6

Author
Lin, Tiffany Gee-Ting

Publication Date
2015

Peer reviewed|Thesis/dissertation

eScholarship.org Powered by the California Digital Library
University of California

UNIVERSITY OF CALIFORNIA,
IRVINE

Microfabricated Platform for the Study of Tunneling Nanotubes

THESIS

submitted in partial satisfaction of the requirements
for the degree of

MASTER OF SCIENCE

in Biomedical Engineering

by

Tiffany Gee-Ting Lin

Thesis Committee:
Professor William C. Tang, Chair
Professor Abraham P. Lee
Assistant Professor Elliot E. Hui

2015

© 2015 Tiffany Gee-Ting Lin

TABLE OF CONTENTS

	Page
LIST OF FIGURES	iii
LIST OF TABLES	v
ACKNOWLEDGMENTS	vii
ABSTRACT OF THE THESIS	viii
CHAPTER 1: Introduction	
Section 1.1: Cell Signaling	1
Section 1.2: Microfabrication for Cell Studies	2
Section 1.3: Current Microplatforms for Cell Studies	3
Section 1.4: Tunneling Nanotubes	5
Section 1.5: Research Work	7
CHAPTER 2: Photolithography	
Section 2.1: Introduction to Photolithography	8
Section 2.2: Positive Photoresist	8
Section 2.3: Negative Photoresist	10
Section 2.4: Chapter Summary	12
CHAPTER 3: Platform Design	
Section 3.1: Design Requirements	13
Section 3.2: Microchannel Platform	14
Section 3.3: Current Methods for Creating Enclosed Microchannels	15
Section 3.4: Mask Design	20
Section 3.5: Chapter Summary	22
CHAPTER 4: Fabrication Processes	
Section 4.1: Substrate Preparation	24
Section 4.2: Partial Exposure Method	26
Section 4.3: Inverted Build Method	32
Section 4.4: Chapter Summary	37
CHAPTER 5: Results and Discussion	
Section 5.1: Introduction	39
Section 5.2: Partial Exposure Method	39
Section 5.3: Inverted Build Method	53
Section 5.4: Chapter Summary	60

CHAPTER 6: Future Work
Section 6.1: PDMS Nanochannels 62
Section 6.2: Enclosed PDMS Nanochannels 66

REFERENCES 73

LIST OF FIGURES

		Page
Figure 1.1	Types of Cell Signaling	1
Figure 1.2	Byrne Microfluidic Device	3
Figure 1.3	Menon Microfluidic Device	4
Figure 1.4	Lee Microfluidic Device	5
Figure 1.5	Tunneling Nanotubes from Rustom	6
Figure 2.1	Metalized Alignment Marks	10
Figure 3.1	COMSOL Rendering of Final Device	15
Figure 3.2	Process Flow from Guerin	17
Figure 3.3	Process Flow from Blanco	18
Figure 3.4	Process Flow from Tuomikoski	18
Figure 3.5	Process Flow from Ceyssens	19
Figure 3.6	312 nm UV Filter	20
Figure 3.7	Layer 1 and Layer 2 Mask Designs	21
Figure 3.8	Overall Mask Design	22
Figure 4.1	Process Flow for UV Filter Characterization	28
Figure 4.2	Process Flow for Partial Exposure Method: 2-Layer 2-Exposure	30
Figure 4.3	Process Flow for Partial Exposure Method: 1-Layer 2-Exposure	31
Figure 4.4	Process Flow for Inverted Build Method: Unexposed Bonding	34
Figure 4.5	Process Flow for Inverted Build Method: Exposed Bonding	35
Figure 5.1	UV Filter Characterization Test Slide	41
Figure 5.2	SU-8 3050 on SU-8 3005	42

Figure 5.3	SU-8 Tests on HMDS-Primed Surfaces	45
Figure 5.4	Microscope Images of Glass Slides with BOE Treatment	47
Figure 5.5	Silicon-Coated Glass Slides	48
Figure 5.6	SU-8 on Silicon-Coated Glass with Metal Alignment Marks	49
Figure 5.7	SU-8 3000 on SU-8 3005	50
Figure 5.8	Microscope Image of 2-Layer Patterned SU-8 on a Silicon Wafer	53
Figure 5.9	Unexposed Bonding Process	54
Figure 5.10	Misaligned Glass from Unexposed bonding Process	55
Figure 5.11	Exposed Bonding Process	56
Figure 5.12	Development of Exposed Bonding Experiment	57
Figure 5.13	Delamination of SU-8 on Silicon Wafer	58
Figure 6.1	AFM-Scanned Surface Profiles	63
Figure 6.2	PDMS Nanochannels	63
Figure 6.3	SEM Images of PDMS Nanochannels	64
Figure 6.4	Cut Attempts on PDMS Nanochannels	65
Figure 6.5	SEM Images of Cut PDMS Nanochannels	66
Figure 6.6	Enclosed PDMS Nanochannels Process Flow	67
Figure 6.7	Enclosed PDMS Nanochannels	67
Figure 6.8	Vibratome Setup	68
Figure 6.9	Cross-Sectional PDMS Slices	69
Figure 6.10	Top View of Enclosed Nanochannels	70
Figure 6.11	SEM Images of Enclosed Nanochannels	71

LIST OF TABLES

		Page
Table 2.1	Properties of SU-8	11
Table 2.2	Processing Steps for SU-8 Layers	12
Table 5.1	Exposure Energy Test Range and Results	40

ACKNOWLEDGMENTS

I would like to thank my advisor and committee chair Professor William Tang for guiding and supporting me in this project during my time as a graduate student at UCI.

I would also like to thank my committee members Professor Abraham Lee and Professor Elliot Hui for sharing their knowledge and suggestions in my research attempts. In addition, a thank you to Dr. Ian Smith for the original challenge and motivation for this project.

Thank you to Carlos Ruiz as my mentor while in the Microbiomechanics Lab for training me and teaching me all of the microfabrication processes, as well as Emily Kha for spending hours with me in the clean room. Without either of them, I would not have been able to conduct my experiments. Also, thank you to Richard Chang and Jake Hes from the UCI Integrated Nanosystems Research Facility for advice and help in using the machinery and tools necessary for this project.

Special thanks to all of the collaborators who have helped to pursue the future direction of the project. Thank you to Cong Wu and Professor Wen Jung Li from City University of Hong Kong for working to create new samples, and Ricardo Albay, Roula Arch, and Professor Charles Glabe for helping to explore the new direction.

I would also like to thank Dr. Yun Yen for encouraging me to pursue the biomedical engineering field and giving me the opportunity to do research.

Thank you to all my friends who have provided tremendous support and encouragement throughout my time in graduate school.

Lastly, I would like to thank my brother Jeffrey and my parents Hwu Rang and Marie Lin for their continued love and support in whatever journey I follow in life.

ABSTRACT OF THE THESIS

Microfabricataed Platform for the Study of Tunneling Nanotubes

By

Tiffany Gee-Ting Lin

Master of Science in Biomedical Engineering

University of California, Irvine, 2015

Professor William C. Tang, Chair

Cell signaling is an integral factor of life that determines important functions for survival. From all types of unicellular to multicellular organisms, cells must communicate between each other in a number of ways through soluble factors in chemical signaling and through cell-to-cell direct contact. A relatively recent discovery of direct juxtacrine signaling is the idea of tunneling nanotubes. These transient connections between cell membranes are formed within minutes and can last for hours, transporting all types of cytoplasmic molecules across these narrow bridges. Tunneling nanotubes are fragile, and very difficult to find in a traditional cell culture environment and in tissue samples. Although many microfabricated platforms exist to study cellular communications, there are no dedicated platforms for the explicit study of these delicate connections.

With this project, we propose the fabrication of an optically clear platform that would allow for the study of tunneling nanotubes. Using negative photoresist SU-8 on a glass substrate, we test various methods to build the platform by limiting UV exposure or by transferring patterned layers between substrates. Despite surface modifications and alternative techniques, we continued to encounter delamination of the layers from the glass

and were ultimately unsuccessful in attempts to fabricate our platform. However, we explore a possible future direction in creating nanochannels by molding PDMS from a nano-indented surface. These nanochannels can then be enclosed by bonding the PDMS to another layer featuring chambers for cell seeding.

CHAPTER 1

Introduction

1.1 Cell Signaling

Communication between cells is a basic necessity for living organisms, from unicellular to multicellular. Cell signals dictate many biological and physiological processes, such as neural transmission and cell proliferation, as well as triggering immune response.

Cell communication can be achieved via soluble factors that allow for chemical signaling or through cell-to-cell contact of synapses or gap junctions [1]. Cell signaling is divided into five major categories: intracine, autocrine, paracrine, endocrine, and juxtracrine. Intracrine involves a cell producing signals within itself, while autocrine signals are secreted outward by a target cell to signal itself. Endocrine signals are transmitted through the blood stream to distant cells, while paracrine signals are sent locally to nearby cells. Juxtacrine signals are sent between two cells that are touching or connected. Figure 1.1 below shows the different type of chemical signaling.

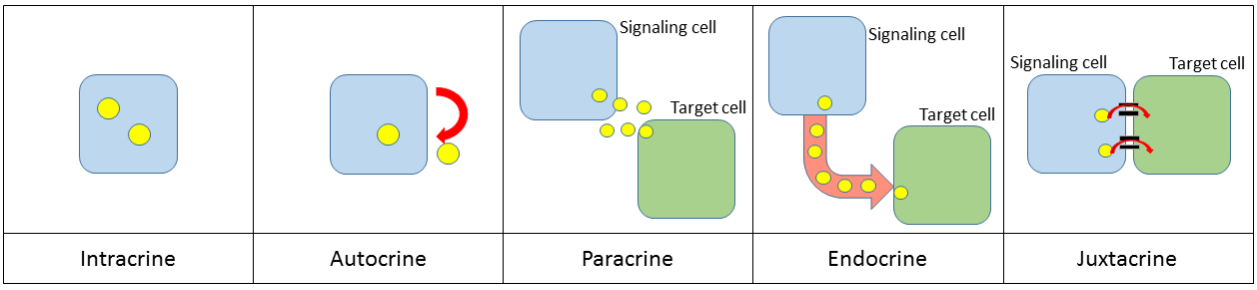

Figure 1.1: Types of Cell Signaling. Intracrine and autocrine signaling is from one cell to itself, with intracrine signals remain inside the cell while autocrine signals are emitted. Paracrine and endocrine signals involve other cells, with paracrine cells being nearby while endocrine signals are transmitted through the bloodstream. Juxtacrine signaling is between adjacent cells.

One way for cells to connect to send juxtacrine signals is through gap junctions. Gap junctions consist of an array of channels that control the flow of ions and biological molecules that pass between two adjacent cells. Surface proteins join the cytoplasms of neighboring cells to form an end-to-end connection of hemi-channels, also known as connexons. These gap junction channels are regulated by membrane voltage, intracellular microenvironment, interaction with other proteins, and phosphorylation [1].

1.2 Microfabrication for Cell Studies

Many platforms have been developed to study cells and cell communications. The advancements in microfabrication and microfluidics allows for many cell-based studies that more similarly recreate the microenvironment of cells than conventional methods on the macro scale. These lab-on-a-chip technologies are miniaturized devices that can allow for controlled factors that can minimizing the amount of resources necessary in experiments.

Microfluidic platforms are often created using soft lithography and elastomer material polydimethylsiloxane, or PDMS, which is an optically transparent material that can easily be bonded to other flat surfaces [2]. Devices made from PDMS must first be shaped from a microfabricated mastermold. The fabrication processes requires the use of a clean room environment to minimize the amount of contamination when creating thin layers and features with dimensions measuring under 50 μm. Since the devices are processed in batch, multiple platforms are fabricated at a time, allowing for minimal use of expensive equipment. While utilizing many common microfabrication techniques, the combination of these steps generates devices without the use of special machinery.

1.3 Current Microplatforms for Cell Studies

Microplatforms are designed to study many types of cell communications between different populations. Some platforms allow for the isolation of cell types to study paracrine signaling, while other devices allow for co-culture of two cell types to study juxtacrine signaling.

Byrne uses microfluidic chambers to study cell signaling via soluble factors. The device features five spaces: three main channels designed to separate signaling molecule lipopolysaccharide, mouse macrophages, and human embryonic kidney cells, and two intermediate channels filled with gel to further isolate the populations. Following a cascade, lipopolysaccharide diffuses through the first separation gel into the second chamber to activate the mouse macrophages, which then releases another signaling molecule that diffuses through the second separation gel to activate green fluorescent protein in the human embryonic kidney cells. Using this platform, concentrations can be tuned in the first chamber to observe changes in fluorescence in the final chamber to study intercellular communication [3]. Figure 1.2 below shows the layout of this device.

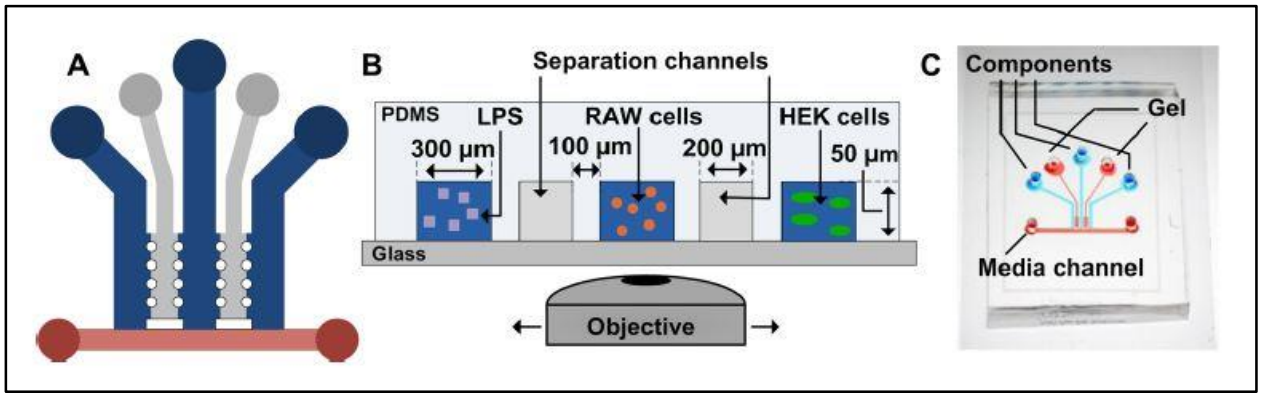

Figure 1.2: Byrne Microfluidic Device [3]**.** A) The microfluidic device features blue channels for samples and grey channels are filled with gel to isolate the sample populations. B) The side view shows the dimensions and spacing of the various chambers. C) The actual device is filled with colored dye to demonstrate the different chambers.

Menon initially separates two cell populations, which can later spread into a common area for co-culture to study cell interactions between bone marrow stromal cells and liver tumor cells. Menon describes a series of steps that selectively plasma treats the outer chambers to create hydrophilic areas for cell seeding, while maintaining a hydrophobic region in between. Hydrophilic properties in the plasma-treated areas are not permanent and hydrophobicity returns to the substrate over time, while the outer chambers remain hydrophilic as a result of gel. Cells cultured in the side chambers can begin to migrate and grow in the intermediate channel for a co-culture environment. Figure 1.3 below shows the steps to prepare the co-culture chip [4].

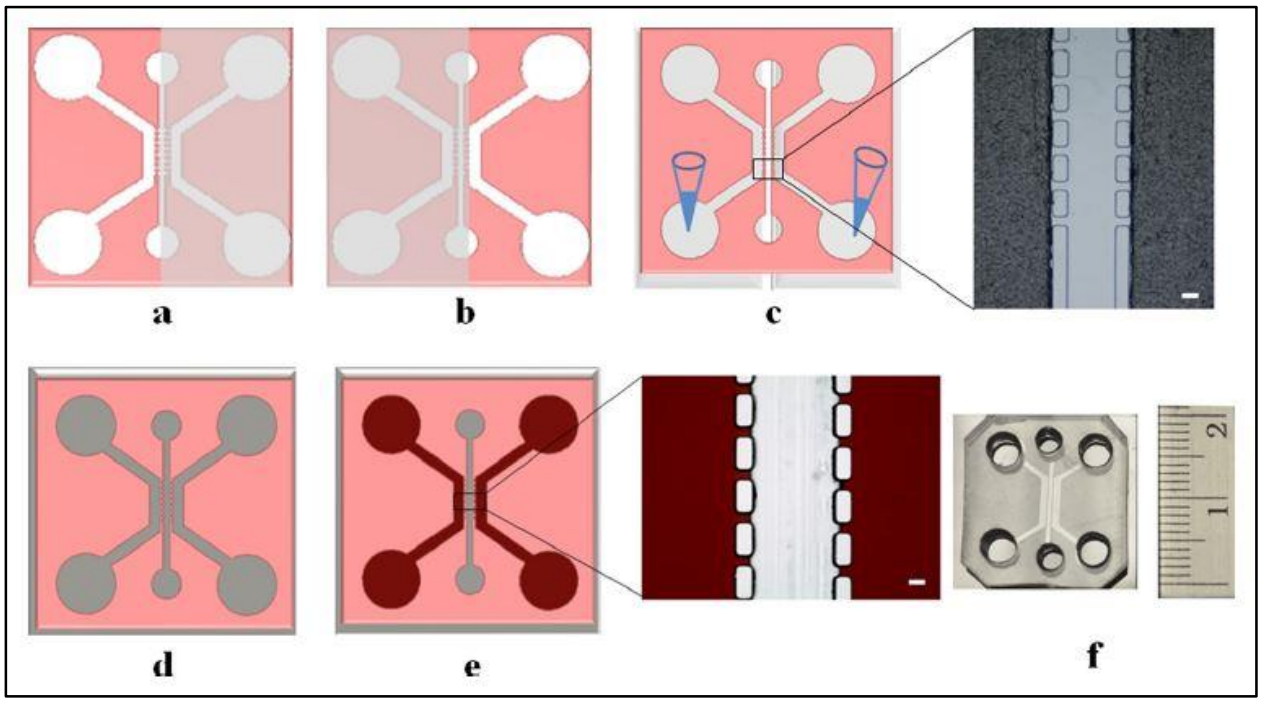

Figure 1.3: Menon Microfluidic Device [4]**.** a) Scotch tape covers the right half of the PDMS device to plasma treat the left side. b) The process is inverted to plasma treat the right side. c) Scotch tape covers the side chambers while leaving the intermediate area open. Gel is introduced into the side chambers to increase wettability. The intermediate channel is shown in a close up. Scale bar = 100μm. d) The PDMS device is bonded to a glass coverslip to complete the sealed chip. e) The chip is dried, and red dye shows that the side chambers remain hydrophilic as a result of the gel while hydrophobicity returns to the center channel. f) The actual microfluidic device is ready for cell culture.

Lee demonstrates the use of a microfluidic device to study gap junctions in mouse fibroblast. The platform captures individual cells along a channel, while aligned channels position a pair of cells to form gap junction. Lee observes the transfer of fluorescent dye from a fluorescently-labeled cell population to a non-labeled population when the individual mouse fibroblast cells experience membrane contact. The fluorescent dye is selected since it is permeable through cell-cell junctions, but cannot diffuse through the plasma membrane of the cell, which demonstrates the functionality of a gap junction. Figure 1.4 below shows the schematic and layout of the microfluidic device [5].

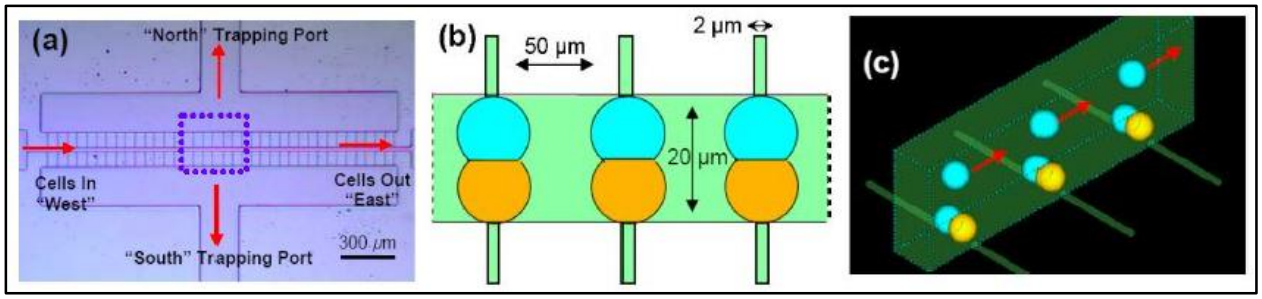

Figure 1.4: Lee Microfluidic Device [5]**.** a) The schematic layout of the microfluidic device, showing that cells flow for "west" to "east," and get trapped in the "north" and "south" trapping ports as a result of pressures applied by fluid flow. b) The drawing shows the dimensions of the trapping area and cells. c) The three-dimensional drawing shows flow of the cells and cells caught in the channel.

1.4 Tunneling Nanotubes

A more recent discovery shows that tunneling nanotubes also offer another mode of juxtracrine signaling between adjacent cells. First discovered in 2004 by Rustom, tunneling nanotubes are a membranous bridge with very small diameters between 20 to 500 nm that connect the cytoplasms of neighboring cells, spanning distances across several cell diameters for several minutes to several hours. Tunneling nanotubes rarely have branched

appearances and formed at the shortest distance between the connected cells. Figure 1.5 below shows the tunneling nanotubes formed by cells in culture [6].

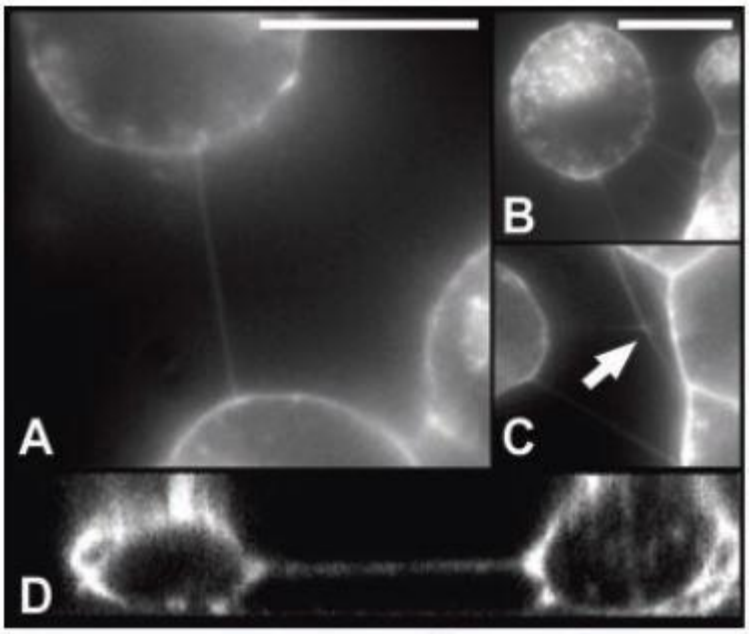

Figure 1.5: Tunneling Nanotubes from Rustom [6]**.** All images show the architecture of tunneling nanotubes formed by rat pheochromocytoma PC12 cells in culture. A) A single nanotube joins two cells. B) Multiple nanotubes are formed between cells. C) Some branching can occur in the nanotubes, as shown by the arrow. D) A selected x-z section from a 3D reconstruction shows the nanotube structure. Scale bars = 15μm.

Tunneling nanotubes can be observed in many different types of cells, including rat pheochromocytoma cells, neurons, myeloid cells, human and murine T cells, rat cardiomyocytes, endothelial progenitor cells, and in various species of bacteria [6]–[8]. They are able to transport different types of cargo, including vesicles derived from various organelles, plasma membrane components, cytoplasmic molecules, ions, or pathogens [7]. The nanotubes can also be formed between species of bacteria, showing to transmit properties of nonhereditary resistance in co-culture [8].

In vitro, these nanotubes are transient connections and very fragile, sensitive to light exposure, shearing force, or chemical fixation [6]. The delicate nature of tunneling nanotubes creates difficulty to further study these cellular connections. In culture, and even more so in actual tissue samples, the tunneling nanotubes are difficult to find and observe.

1.5 Research Work

In this work, we propose a platform created from microfabrication techniques designed to study tunneling nanotubes. Although many current platforms study cell communications on a microscale, microfluidic chambers are too large to study individual cells and the nanotubes formed between them. This device would allow for specific placement of cells, which are separated by walls with designated openings for the formation of the nanotubes. The goal of the platform is to more easily pinpoint a location of tunneling nanotubes if they were to form between isolated cells. This device would facilitate imaging and analysis of tunneling nanotubes to learn more about the properties of these transient connections.

CHAPTER 2

Photolithography

2.1 Introduction to Photolithography

Photolithography is a common method used in microfabrication that allows for the transfer of a designed pattern through the use of a photoresist and UV light. A black and clear mask selectively allows light to reach the photoresist, and the uncrosslinked portions of the resist are removed in developer. The reproducibility of this pattern onto substrates is commonly used to create computer circuit boards. It can also be used to create molds for microfluidic channels and selectively pattern metal.

Basic procedure steps for photolithography include cleaning a substrate, spin coating of a photoresist, exposing the photoresist to UV light through a mask to create a pattern, and developing the photoresist to reveal the patterned design.

There are two categories of photoresist: positive and negative. Positive photoresist, when exposed to UV light, becomes soluble in developer solution. Conversely, negative photoresist becomes crosslinked when exposed to UV light, becoming insoluble to developer.

The majority of the project focuses on the use of negative photoresist SU-8, but positive photoresist SC1827 is also used for certain aspects in the fabrication processes.

2.2 Positive Photoresist

For this project, Microposit SC1827 (MicroChem), also known as Shipley, is used for our positive photoresist needs. Briefly, the processing steps for SC1827 are as followed. The

cleaned substrate is placed into a spin coater (Laurell Technologies Corp.), and a puddle of SC1827 is poured into the center. The spin cycle is done in two steps: a 10-second spin at 500 rpm with an acceleration of 300 rpm/s, followed by a 30-second spin at 3500 rpm with an acceleration of 500 rpm/s. This results in a 20μm-thick layer of SC1827, which then must be soft baked at 90°C for 10 minutes. To pattern the photoresist, it is exposed to UV energy of 250 mJ/cm^2 and subsequently developed for approximately 2 minutes in developer solution Microposit MF-319. Water is then used to stop the developing process and rinse the substrate. Overdevelopment could remove our desired patterned features, while underdevelopment would leave photoresist in areas that should be clear [9].

2.2.1 Fabrication of Alignment Marks

For some testing experiments, it was necessary to fabricate metal alignment marks using a lift-off technique. This process is done by spin coating positive photoresist SC1827 onto the substrate, and exposing the photoresist with the alignment pattern. As a positive photoresist, the light crosslinks the photoresist to weaken it and make it susceptible to be washed away in developer solution. The exposed SC1827 pattern is developed in MF-319 developer solution. The substrate is then coated with metal using an e-beam evaporator. The substrate is submerged in acetone to "lift-off" the underlying photoresist, leaving behind the desired metal alignment features on the substrate [10]. Having metalized alignment marks allows for better visualization when using the mask aligner to expose patterns together. Although it is possible to fabricate two-layered SU-8 without metalized alignment marks, it is more difficult when other layers of materials are added into the process. As shown below

in Figure 2.1 inside the red box, small crosses of different sizes serve as alignment marks that will assist in the fabrication of future layers.

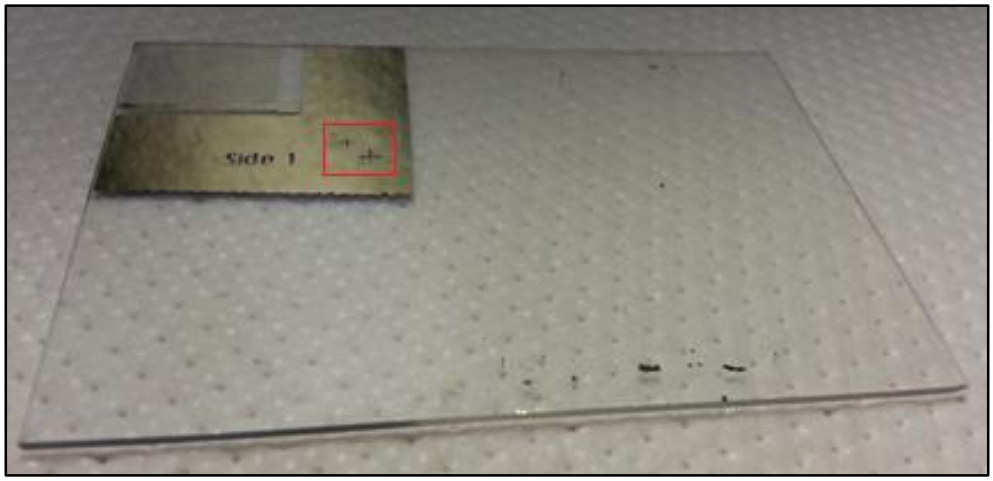

Figure 2.1: Metalized Alignment Marks. Alignment marks are first patterned using positive photoresist SC1827, and metal is coated on top using an e-beam evaporator. Unwanted metal is lifted off when the slide is submerged in acetone.

2.3 Negative Photoresist

The bulk of this project is done using negative photoresist SU-8. It is an epoxy-based photoresist that is often used in microfabrication. It is capable of forming tall structures with a high aspect-ratio, and it is also chemically inert, mechanically stable, and optically transparent [11]. There are different types of SU-8, each with different viscosities that are able to achieve various ranges of heights. The more viscous SU-8 types are used to build thicker structures, while less viscous SU-8 types are needed to produce thin layers of less than 10μm. Table 2.1 below tabulates the manufacturer's information of percentage of solids, viscosities, and densities for the corresponding types of SU-8 (MicroChem) used for this project.

SU-8 Type	% Solid	Viscosity (cSt)	Density (g/ml)
2	---	45	---
2002	29	7.5	1.123
2010	58	380	1.187
2050	71.65	12900	1.233
3005	50	65	1.075
3050	75.5	12000	1.153

Table 2.1: Properties of SU-8. The table shows the % solid, viscosity, and density of the different formulations of SU-8 used for this project [12]–[15].

The original SU-8 resists are formulated in a gamma butyrolactone solvent, but the newer SU-8 2000 and 3000 series are formulated in an updated cyclopentanone solvent to improve coating and adhesion properties [11]. SU-8 2000 series also differs from SU-8 3000 series. The 2000 series is able to create thicker layers with a higher aspect ratio of 10:1 with faster drying times, while the 3000 series can only achieve an aspect ratio of 5:1, but offers better adhesion to substrates [14], [15].

Procedural steps for SU-8 are similar to that of positive photoresist SC1827. A cleaned substrate is loaded into a spin coater for a two-step spin cycle, and a puddle is poured into the center of the substrate. The distributed layer undergoes a soft bake procedure to remove some of the solvent before being exposed with a pattern. Unlike the positive photoresist, the SU8 needs to undergo a Post Exposure Bake (PEB) step to further remove solvent before the pattern can be developed in SU-8 developer (MicroChem) [14]. Specific spin recipes, bake times, and exposure dosages are tabulated below in Table 2.2 for the different types of SU8 and desired thicknesses.

SU-8 Type	Thickness	Spin Recipe	Soft Bake	Exposure	Post Exposure Bake	Development
2	4 μm	500 rpm for 10s acceleration at 100rpm/s 1000 rpm for 30s acceleration at 300rpm/s	1 min at 65°C 3 min at 95°C	80 mJ/cm^2	1 min at 65°C 1 min at 95°C	1 min
2002	2 μm	500 rpm for 10s acceleration at 100rpm/s 3000 rpm for 30s acceleration at 300rpm/s	1 min at 95°C	80 mJ/cm^2	2 min at 95°C	1 min
2002	2.9 μm	500 rpm for 10s acceleration at 100rpm/s 1000 rpm for 30s acceleration at 300rpm/s	1 min at 95°C	90 mJ/cm^2	2 min at 95°C	1 min
2010	10 μm	500 rpm for 10s acceleration at 100rpm/s 3500 rpm for 30s acceleration at 300rpm/s	3 min at 95°C	125 mJ/cm^2	4 min at 95°C	3 min
2050	50 μm	500 rpm for 10s acceleration at 100rpm/s 3250 rpm for 30s acceleration at 300rpm/s	3 min at 65°C 7 min at 95°C	160 mJ/cm^2	2 min at 65°C 6 min at 95°C	6 min
2050	60 μm	500 rpm for 10s acceleration at 100rpm/s 2500 rpm for 30s acceleration at 300rpm/s	3 min at 65°C 7 min at 95°C	180 mJ/cm^2	2 min at 65°C 7 min at 95°C	7 min
2050	120 μm	500 rpm for 10s acceleration at 100rpm/s 1500 rpm for 30s acceleration at 300rpm/s	5 min at 65°C 20 min at 95°C	250 mJ/cm^2	5 min at 65°C 10 min at 95°C	11 min
3005	10 μm	500 rpm for 10s acceleration at 100rpm/s 1000 rpm for 30s acceleration at 300rpm/s	3 min at 95°C	200 mJ/cm^2	1 min at 65°C 2 min at 95°C	3 min
3050	50 μm	500 rpm for 10s acceleration at 100rpm/s 3000 rpm for 30s acceleration at 300rpm/s	15 min at 95°C	250 mJ/cm^2	1 min at 65°C 5 min at 95°C	8 min

Table 2.2: Processing Steps for SU-8 Layers. The table shows the corresponding spin recipes, soft bake time, exposure energy, post exposure bake time, and development time required to achieve layers of specific thickness using the corresponding formulations of SU-8. Exposure energies are tabulated for a 1x on a silicon wafer. For exposure on a glass substrate, exposure energies must include a 1.5x multiplication factor [12]–[15].

2.4 Chapter Summary

Photolithography is a useful method to create patterns on a small scale through the use of photoresists and UV light. Positive photoresist degrades when exposed to light, while negative photoresist crosslinks and hardens when exposed to light. In this project, positive photoresist SC1827 is used to create alignment marks, while negative photoresist SU-8 serves as the main structural component of this platform. Photoresist requires a series of processing steps to create each patterned layer, including a spin coat, exposure, and development, along with intermediate baking steps depending on the type of photoresist. The use of traditional photolithography methods and the combination of both positive and negative photoresists are used in the fabrication of this proposed platform of enclosed microchannels.

CHAPTER 3

Platform Design

3.1 Design Requirements

The purpose of the project is to design a platform that would allow for the study of tunneling nanotubes created by cells as a means for communication. Given this challenge, there are four major design concerns and requirements when designing the platform.

Firstly, the fabrication process would need to be capable of creating structures within the same order of magnitude as cells and the tunneling nanotubes. Microfabrication processes can be done with many different materials and metals that can be patterned precisely at the micro scale.

Secondly, the materials used for the platform must be biocompatible. Cells need to be able to adhere to the surface of the platform. Although proteins can be deposited onto various substrate surfaces to allow for cellular adhesion, some materials are still not compatible to these proteins and would therefore not be suitable for this project.

Thirdly, the platform needs to be optically clear to be able to visualize the cells and the resulting nanotubes with the use of an upright microscope. If the material used for the devices are opaque, then there would be no possible visualization of features without destroying either the device or the cells.

Lastly, the platform requires the isolation and separation of individual cells. The enclosure space must be large enough to place an individual cell with ample surrounding media to keep the cell viable throughout the duration of the experiment, but a gap space needs to be available for cells to form these nanotubes. Since we also want to test how far

these nanotubes span, we also need to create various separation distances between these single-cell enclosures.

3.2 Microchannel Platform

The proposed platform would feature an array of enclosed microchannels made from SU-8 on a glass substrate. SU-8 serves as the structure material, with gap spaces serving as enclosed channels for nanotube formation between cells on either side of the channel. The microchannels would have a width of 500nm, which is the maximum value of the range of nanotube diameters, according to Rustom [6]. We create four lengths of channels of 1, 3, 5, and 7μm to test the span of the nanotubes. Although the nanotubes are capable of spanning multiple cell diameters, we begin with shorter distances. The height of the channel would be between 5μm and 10μm, which is approximately the size of cells. This dimension is also more feasible to create and pattern using our SU-8 material.

Since many different types of cells form tunneling nanotubes, some cell diameters may exceed the 10μm height of the channel. By enclosing the microchannels with a 50μm wall of SU-8, larger cells would be isolated and only able to form nanotubes in our predetermined gap space.

This platform allows for better visualization of the tunneling nanotubes by limiting the space for which cells can form these connections. The overall schematic of the platform is shown in a COMSOL rendering in Figure 3.1 without the glass substrate base.

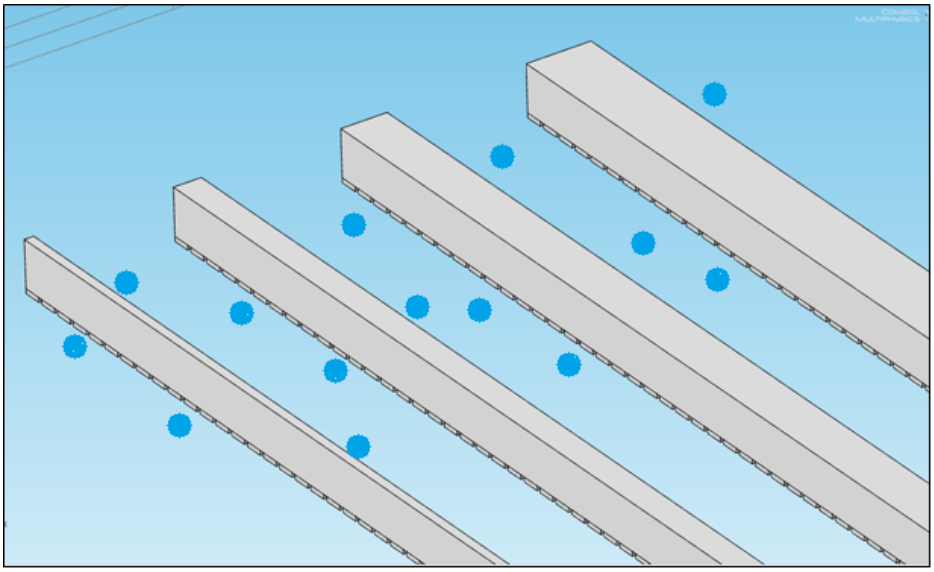

Figure 3.1: COMSOL Rendering of Final Device. This demonstrates what the overall device would look like, with a thin layer of SU-8 blocks underneath a larger block. Blue circles represent where cells would be located in the device, and cells can form tunneling nanotubes through the channel space underneath the larger walls.

3.3 Current Methods for Creating Enclosed Microchannels

The use of SU-8 on a glass substrate seems ideal for the construction of such a platform. As mentioned earlier in Section 2.3, SU-8 is chemically inert and optically transparent and can be fabricated on glass using standard photolithography techniques [14]. Currently, there are a few methods for fabricating enclosed microchannels using photoresists.

The first method would be to pattern the first layer of SU-8 and fill in the gaps with a sacrificial material that can be later removed, after the top enclosing layer is created and patterned. Known as the "fill-process," Guerin tests thermoplastics, waxes, and epoxies as potential filling materials [16]. One of the main issues is finding an appropriate material that can completely fill the voids. Also, any extra material deposited could overflow and influence the patterning of our top layer of SU-8. SU-8 solvent would also dissolve most materials [14].

This method did not seem appropriate and applicable for our project, as possible sacrificial materials were not compatible with other design requirements.

Guerin also tests using a "mask-process," which involves a patterned metal coating on top of the first layer of SU-8 to protect it from being crosslinked when subsequent layers of SU-8 are built on top. The metal layer remains in the construct, which would not fit with the design requirement of being optically clear. Both of these methods are demonstrated in a process flow as shown below in Figure 3.2.

The second method involves patterning the two layers on separate substrates, and bonding the two together after proper alignment. Blanco brings fully developed SU-8 layers in contact above the glass-transition temperature, and later releases the silicon wafer substrate to create the desired SU-8 device as a result of a buffered oxide etch [17]. This method is demonstrated in the process flow below in Figure 3.3.

Another approach would also be to bring a fully exposed layer of SU-8 in contact with an unexposed SU-8 layer on a glass slide. After bonding, the unexposed SU-8 layer can be exposed through the backside of the glass to complete the bond to the other layers. This method also requires a buffered oxide etch step to release the silicon wafer substrate and complete sacrifice of the glass. The process flow is shown below in Figure 3.4 [18].

The third method involves limiting certain wavelengths to selectively expose only the top portion of the SU-8 layer instead of penetrating all the way to the substrate [19]. MicroChem suggests exposures require a use of a low-pass filter to eliminate wavelengths under 350 nm to prevent unwanted T-shaped walls [14]. However, Ceyssens uses a 313 nm wavelength of light to create overhanging structures of SU-8, as shown in Figure 3.5 [19].

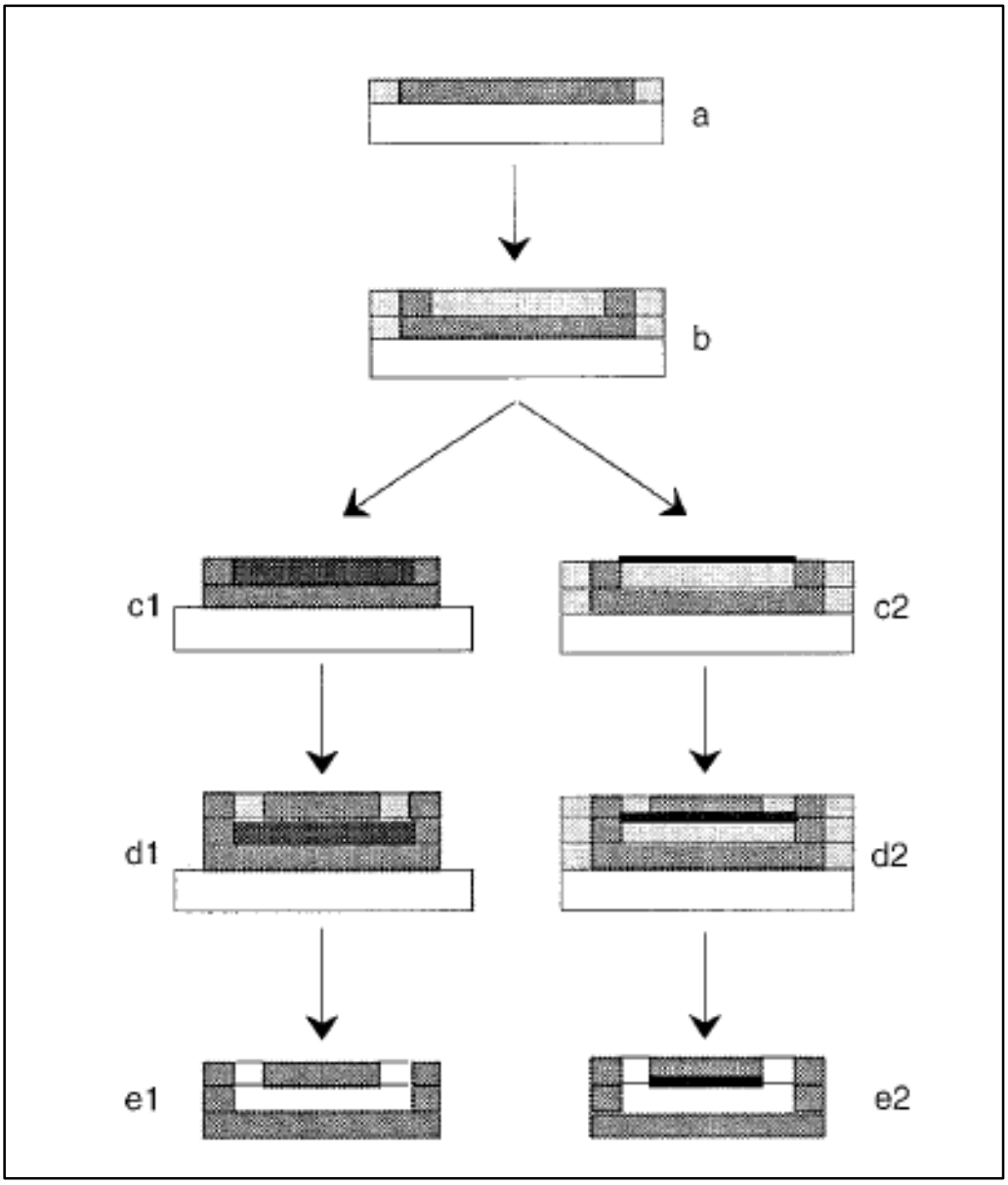

Figure 3.2: Process Flow from Guerin [16]**.** a) A single layer of SU-8 is coated onto the substrate and patterned normally. b) A second layer is spin coated on top and patterned to form side walls. Left: fill process. c1) After the construct is developed, a filling material is put into the cavity. d1) the following layer of SU-8 is coated and patterned. e1) The construct is developed, and the filling material is removed to reveal the enclosed channel. Right: mask process. c2) A metal mask is patterned to prevent light from penetrating to the unexposed region. d2) The next layer of SU-8 is processed and patterned on top of the mask. e2) The construct is developed, and the mask remains in the construct. (Light grey: noncrosslinked SU-8; Middle grey: crosslinked SU-8; Dark grey: filling material; Black: metal.)

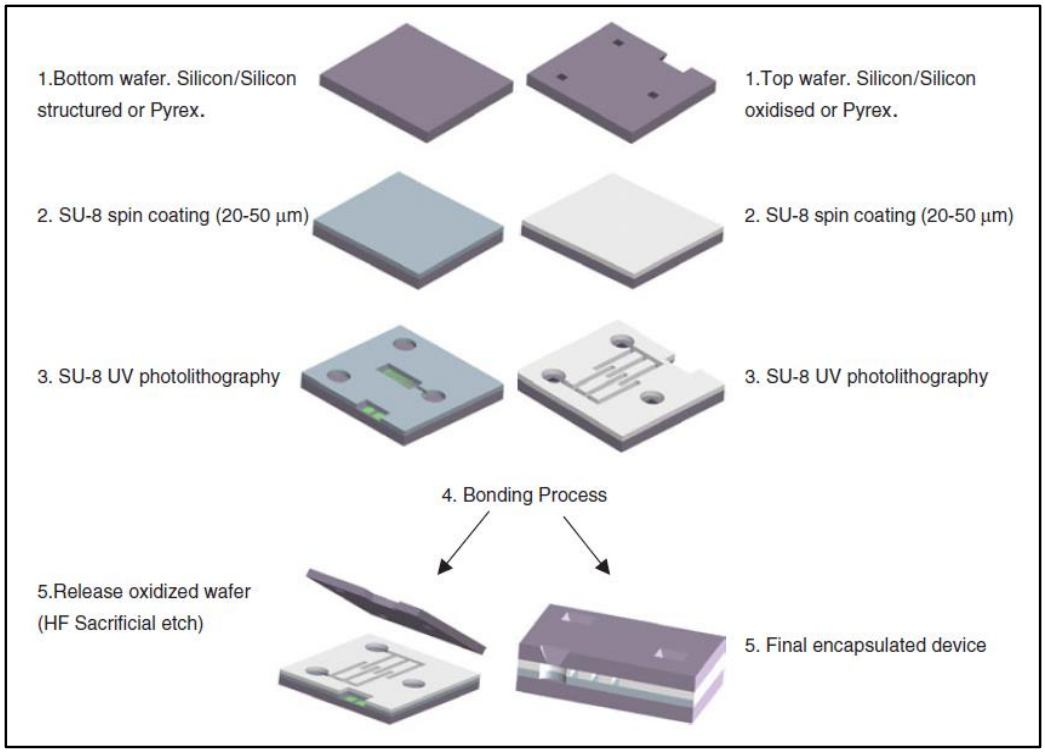

Figure 3.3: Process Flow from Blanco [17]**.** This process flow demonstrates the patterning of two layers of SU-8 on two different substrates. The layers are then bonded together to create a final enclosed device, or the substrates can be removed using a HF sacrificial etch.

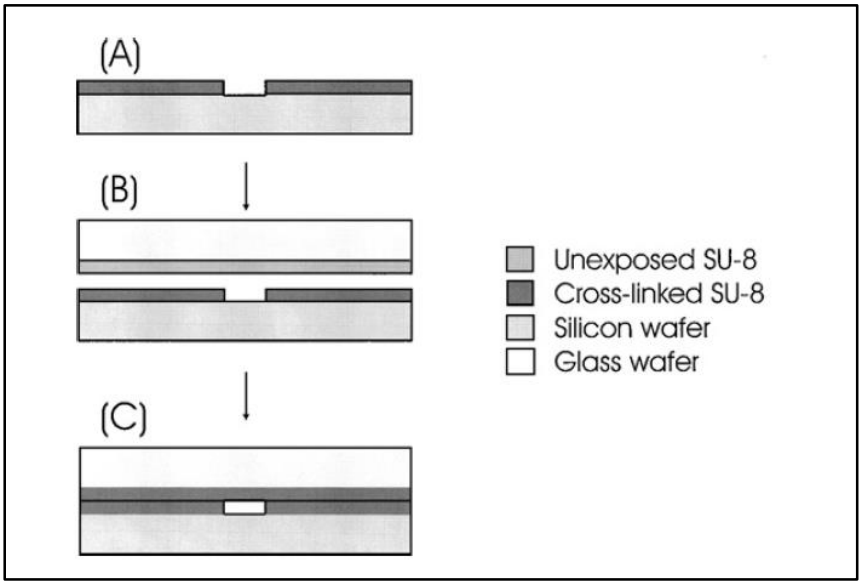

Figure 3.4: Process Flow from Tuomikoski [18]**.** A) The first layer of SU-8 is patterned onto the silicon wafer. B) An unexposed layer of SU-8 on a glass slide is bonded to the crosslinked layer of SU-8 on the wafer. C) The SU-8 is then exposed through the backside of the glass to complete the bond and create an enclosed microchannel.

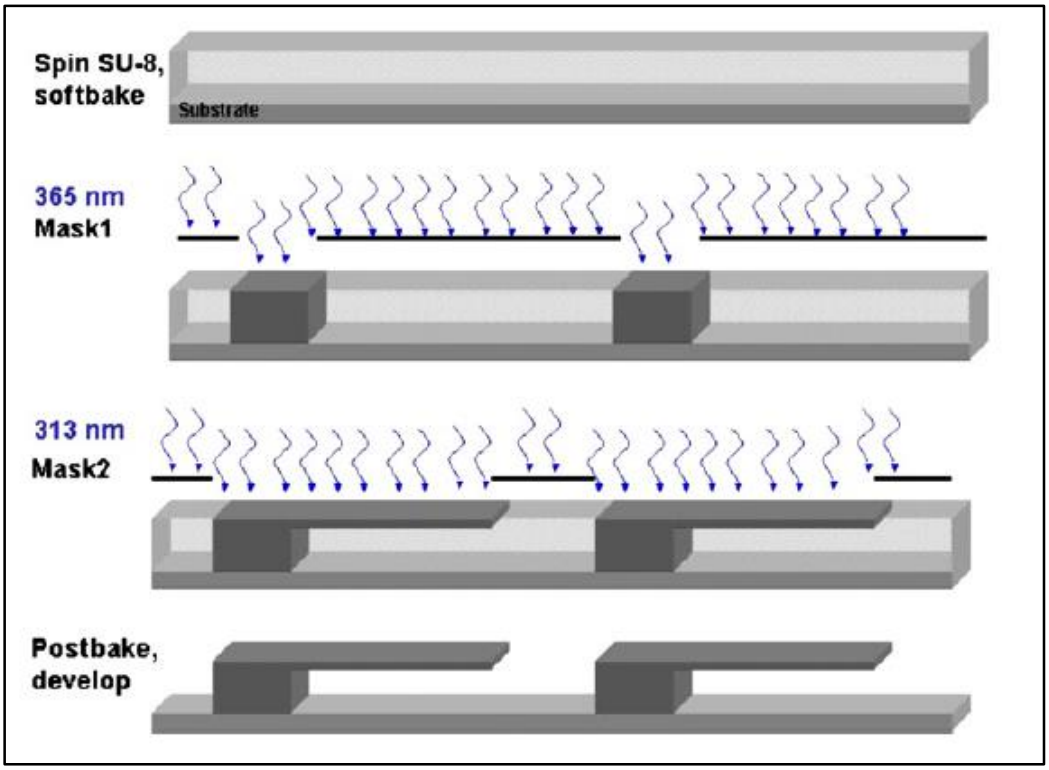

Figure 3.5: Process Flow from Ceyssens [19]**.** The process begins with a layer of SU-8 that is spin coated and soft baked on a substrate. Using normal UV light, the first base pillars are exposed and patterned. Then, using a different wavelength of light, the overhanging platforms are exposed without completely exposing to the substrate. The final device undergoes a post exposure bake and subsequent development step to reveal final cantilevers.

3.3.1 Summary of Current Methods

These proposed processes result in microchannels on a silicon wafer, which would not be suitable for our applications and does not meet our design criterion of being optically clear. The fill method proposed by Guerin would not work without a proper sacrificial material, and the mask method would leave behind the metal mask layer that would not satisfy the optically clear requirement.

The methods proposed by Blanco and Tuomikoski can leave behind a freestanding device without any substrate support, but the procedure can be modified for our platform,

since we would ideally like to maintain the glass as a support for the fragile SU-8 construct. The partial exposure theory by Ceyssens seems like the best option to test for the fabrication of our device. We purchased an optical UV bandpass filter centered at 312 nm with a full width at half maximum of 50 nm (Omega Optical) to provide us with a lower range of wavelengths. The UV filter is shown below in Figure 3.6.

Figure 3.6: 312 nm UV Filter. The UV Filter is a small circular disc that is placed on top of our pattern, limiting the wavelengths of light that will expose the pattern on the SU-8 layer.

3.4 Mask Design

For both test methods of using a filter and bonding separate layers together, the same mask design can be used for the fabrication processes. The mask features two different designs, which would align together to create our enclosed channel spaces.

The Layer 1 mask would create an array of rectangular blocks, leaving a 500 nm gap width of space for nanotube formation. The rectangles have varying sizes of 1, 3, 5, and 7μm to test if the nanotubes are able to span the length of this channel. The thickness of the first layer of SU-8 would provide the height dimension of our proposed enclosed channel. The

Layer 2 mask is designed to match the width of the Layer 1 rectangles and form a thicker vertical wall to separate the cells. To create smaller chips for increased throughput, each 4-column section is repeated within a 15 mm square, which can also fit under the area of our UV filter. Figure 3.7 shows a zoomed in look at the Layer 1 and Layer 2 mask designs.

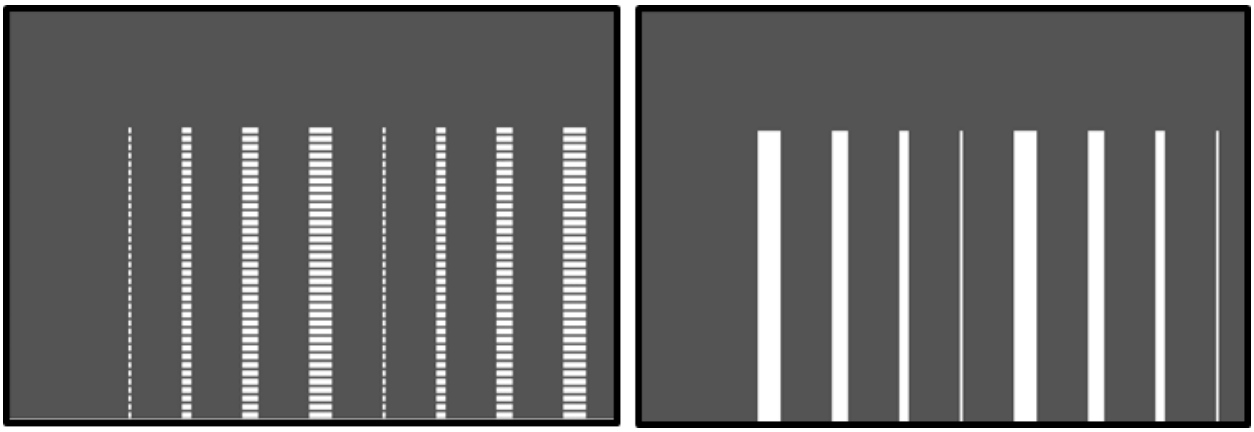

Figure 3.7: Layer 1 and Layer 2 Mask Designs. (Left) Layer 1 Mask design shows a repeated pattern of four columns, with sizes of 1, 3, 5, and 7 μm with a 500nm gap space between the blocks in the column. (Right) Layer 2 Mask shows the corresponding 7, 5, 3, and 1 μm columns that would overlay and align with Layer 1 Mask when the mask is rotated.

By ordering a chrome hard mask on a 5-inch square, we can fit six repeated patterns each of Layer 1 and Layer 2 that would fit on a single 4-inch wafer. We designed the layout so that Layer 2 can easily align to Layer 1 by rotating the mask, with the help of alignment marks. The plus-sign shapes alignment marks generated from Layer 1 fit within the outline on the Layer 2 mask alignment marks. The final completed design should create long strips made from Layer 2, but Layer 1 creates the gap spaces that would allow for the nanotubes to form. The overall mask design is shown in Figure 3.8.

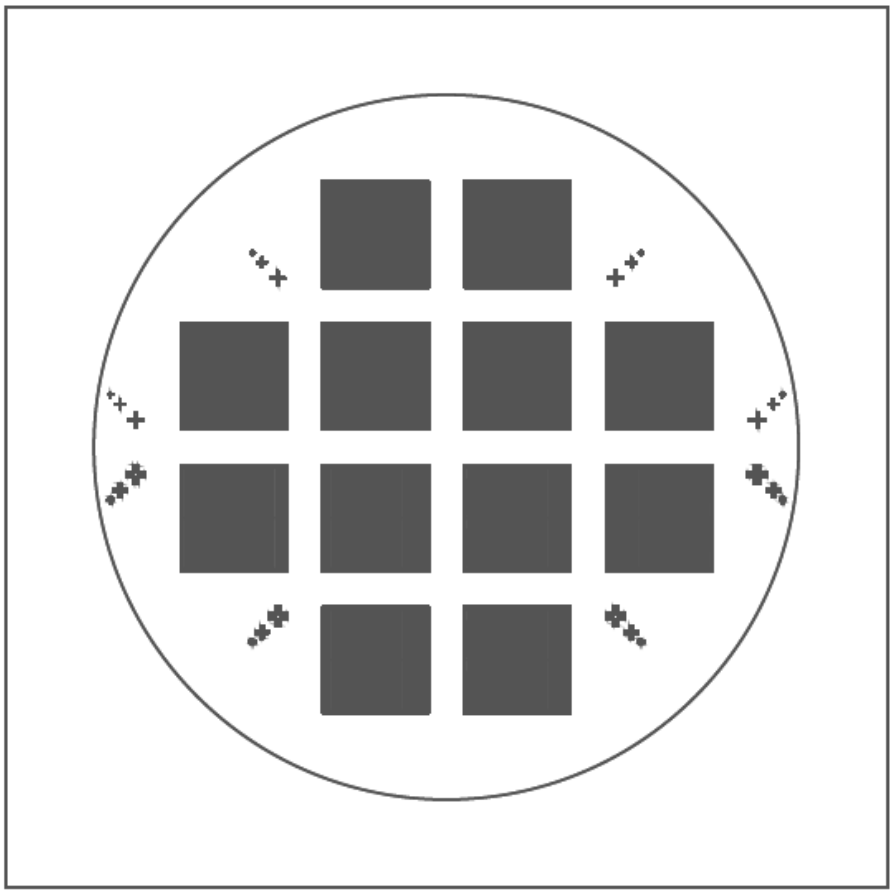

Figure 3.8: Overall Mask Design. The overall hard mask design, featuring six squares of Layer 1 Mask on the top half and six squares of Layer 2 Mask on the bottom half. The mask is designed so that Layer 2 designs can directly lay on top of Layer 1 after a rotation and proper alignment, with the help of the alignment marks.

3.5 Chapter Summary

For this device, we are challenged to create an optically clear and biocompatible platform, featuring an array of enclosed channels for cells to form tunneling nanotubes. By creating an SU-8 structure to limit space where nanotubes can form, we would be able to better locate and visualize these connections. Current methods for the fabrication of enclosed channels are proposed by Guerin, Blanco, Tuomikoski, and Ceyssens. Both the fill process and mask process by Guerin would not be suitable for our fabrication process.

Blanco and Tuomikoski both form enclosed channels the bonding of two separate layers, which can be modified for our platform. The best option is to modify the partial exposure method by Ceyssens to create our enclosed channels. For both the bonding or partial exposure methods, we can use the same mask design that features a Layer 1 pattern of small individual blocks and a Layer 2 pattern with larger strips. With a single hard mask design, we can create multiple chips and easily align the two layers to create our enclosed channels.

CHAPTER 4

Fabrication Processes

4.1 Substrate Preparation

The first step in preparing for microfabrication is to properly clean the substrate. Since these processes involve dangerous chemicals, extra protective gear must be worn while performing these cleaning procedures inside a clean room environment. Users need to wear thick nitrile gloves, a chemical apron, and a safety shield to handle chemicals. Wafers are usually cleaned with a hydrofluoric acid (HF) dip, and glass is cleaned using either RCA1 or piranha solution.

4.1.1 HF Dip

For SU-8 on a silicon wafer substrate, the cleaning step requires dipping the substrate in 2% HF. This step removes the silicon dioxide layer that naturally forms on the silicon wafer to improve adhesion of SU-8 [20]. The buffered HF solution is poured into a polypropylene beaker, and a silicon wafer is allowed to soak for a few minutes. The wafer is then removed and thoroughly rinsed under running DI water. The oxide layer is completely removed when the surface is no longer hydrophilic and the water beads off, since pure silicon is naturally hydrophobic. Samples are then dried using nitrogen gas. HF solution is reusable, and it is stored in a polypropylene container within the proper chemical safety containers. The hydrophobicity of the wafer allows for better SU-8 adhesion. However, the HF dip is not necessary for all applications, especially if the SU-8 structures are intended to be removed from the wafer.

4.1.2 RCA-1 Clean

RCA-1, also known as a standard clean-1 or SC-1, is a process that removes organic residues and films from a substrate. It can be used to clean silicon wafers, but we use this cleaning process for glass substrates. The process involves a recipe of 5 parts of water, 1 part of 27% ammonium hydroxide (NH_4OH), and 1 part of 30% hydrogen peroxide (H_2O_2) [21]. Generally, 325 ml of water is poured into a Pyrex beaker and combined with the 65 ml of ammonium hydroxide. The combined solution is heated on a hot plate to approximately 75°C, and 65 ml of hydrogen peroxide is then added to complete the solution. Glass slides are allowed to soak for 15 minutes. Slides are then transferred to another beaker for rinsing under running DI water for another 5 minutes before samples are dried with nitrogen gas. RCA-1 solution is still effective while hot, so remaining solution should be allowed to cool overnight and disposed with base waste.

4.1.3 Piranha Clean

A piranha clean is similar to that of RCA-1 but can be applied to a wider selection of materials. The standard recipe for a piranha solution is three parts of 98% sulfuric acid (H_2SO_4) and one part of 30% hydrogen peroxide (H_2O_2) [22]. Generally, 150 ml of sulfuric acid is poured into a Pyrex beaker and heated to 80°C. Next, 50 ml of hydrogen peroxide is slowly poured into the heated sulfuric acid, causing an exothermic reaction that causes bubbling and heats the combined solution to approximately 100°C. The solution should be maintained on the hot plate between 100°C and 110°C while glass slides are allowed to soak in the solution for 20 minutes. The slides are then removed and allowed to soak under running DI water for five minutes, before being moved to another water rinse beaker for an

additional two minutes. Glass slides are then removed and dried with nitrogen gas. Similar to RCA-1, the solution is reusable while hot, so it must also be allowed to cool overnight. Piranha solution is then disposed with the appropriate acid waste.

4.1.4 Summary of Substrate Preparation

Both RCA-1 and piranha cleaning processes are very similar, with piranha solution being more dangerous than RCA-1 due to its exothermic reaction caused by the mixing of sulfuric acid and hydrogen peroxide. Piranha solution also removes metal contamination. RCA-1 needs to be heated to the proper temperature before a reaction occurs. RCA-1 also has more water content, so it is kept below boiling as to avoid too much evaporation of the solution. These glass slides are required for all of the subsequent SU-8 processes, so no specific tests were used solely to test adhesion after the different cleaning procedures. After the first round of RCA1-cleaned slides were used, we attempted to see if piranha-cleaned glass would have any improvements. There was no noticeable difference in results, but glass slides were cleaned using piranha solution for all future experiments.

4.2 Partial Exposure Method

The partial exposure method is based on a protocol from Ceyssens which uses a UV filter to limit the wavelengths that reach the surface of the substrate [19]. The partial exposure method is divided into two tests: a 2-layer 2-exposure technique, or a 1-layer 2-exposure technique.

4.2.1 UV Filter Characterization

To properly use the UV filter, it first needs to be characterized so we can achieve the appropriate depths of exposure. A layer of SU-8 is spin coated onto a glass slide and soft baked as usual. A large block pattern is exposed through the backside of the glass. Exposing through the backside would allow for the base of the SU-8 touching the glass to be exposed first, creating an attachment to the substrate. Each block pattern is exposed at a test dosage of energy through the UV filter, while the remaining area of glass is covered using aluminum foil to prevent accidental exposure to the unexposed SU-8. After exposure, the entire glass slide continues to the PEB time specified in Table 2.2 and then proceeds to the subsequent development step.

Increased exposure energies would result in thicker layers of SU-8, which can be measured using a surface profilometer. The profilometer takes a stylus point and traces across the surface, rising and falling with the surface of the SU-8 to provide a measurement. The area of the 1in x 3in glass slide is divided into five spaces, which allows for four test dosages through the filter and a non-filtered control. This can also be replicated on a 2 in x 3 in glass slide, with seven test dosages. This allows us to test a range of exposure energies to correlate with a height of SU-8, as shown below in Figure 4.1. Since different SU-8 types require different exposure energies, the characterization is only performed on SU-8 2050, which we use to create thick 50μm layers.

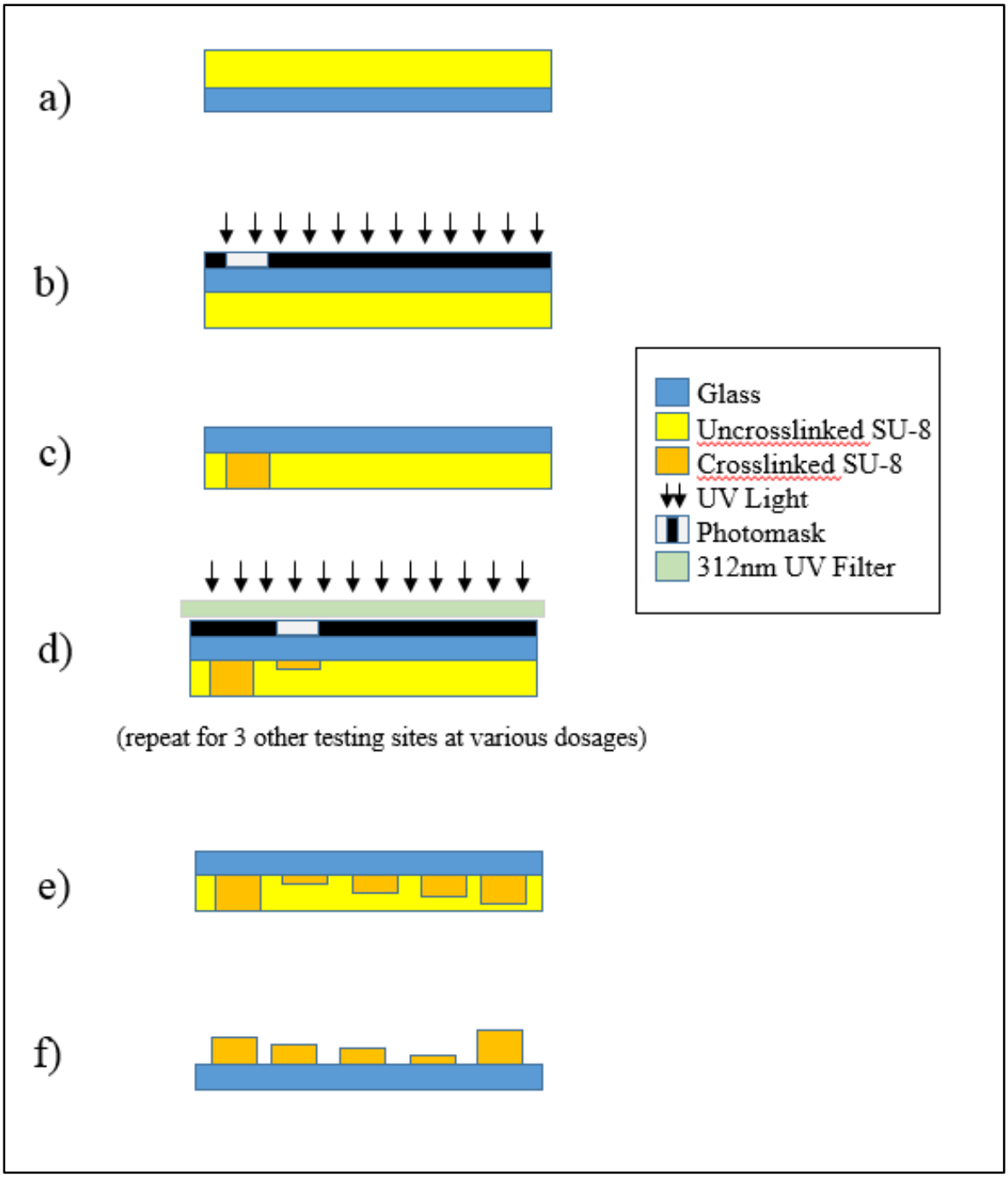

Figure 4.1: Process Flow for UV Filter Characterization. a) The SU-8 is first spin coated onto a clean glass substrate. b) The first block pattern is exposed through the backside of the glass without a filter to serve as a control. c) The control site patterned in the SU-8. d) This step is repeated for each test location, varying the energy dosage exposed through the UV filter. e) The resulting SU-8 structures which need to undergo a PEB step. f) The final structure produced after development, which can then be measured using a surface profilometer.

4.2.2 Experiment: 2-Layer 2-Exposure

The first method for forming these microchannels required two layers of SU-8, each being exposed separately. After the substrate is properly cleaned, it is dehydrated in a 120°C oven for over two hours to ensure the surface is free of moisture for the first SU-8 layer. The first layer is a 10μm layer, which is made using either SU-8 3005 or SU-8 2005. Corresponding spin recipes are found in Table 2.2. This first layer is exposed with Layer 1 mask and followed by the PEB step, which allows for visualization of the exposed pattern. Without development, the subsequent 50μm layer is then spin coated on top of the first layer using SU-8 2050. The thicker layer is then exposed through the filter using the MA6 mask aligner to ensure that the top Layer 2 features align with the Layer 1 features. The second layer undergoes PEB, and both layers are developed together in SU-8 developer solution. The step-by-step procedure is shown below in Figure 4.2.

4.2.3 Experiment: 1-Layer 2-Exposure

The second method of partial exposures features one thicker layer of SU-8 that undergoes two separate exposure steps. Similar to the previous method, this procedure also begins with a dehydration bake. However, this SU-8 layer is a single 60μm layer made from SU-8 2050. Layer 1 is exposed completely through the 60 μm layer using the mask aligner to simplify the exposure of the Layer 2. There is no PEB step after the first exposure, and Layer 2 is immediately exposed through the filter to achieve the 50μm layer. The entire construct undergoes PEB and is then developed in SU-8 developer. This 1-layer 2-exposure procedure is shown below in Figure 4.3. This figure also features the processing of the optional surface modification of an SU-8 adhesion layer.

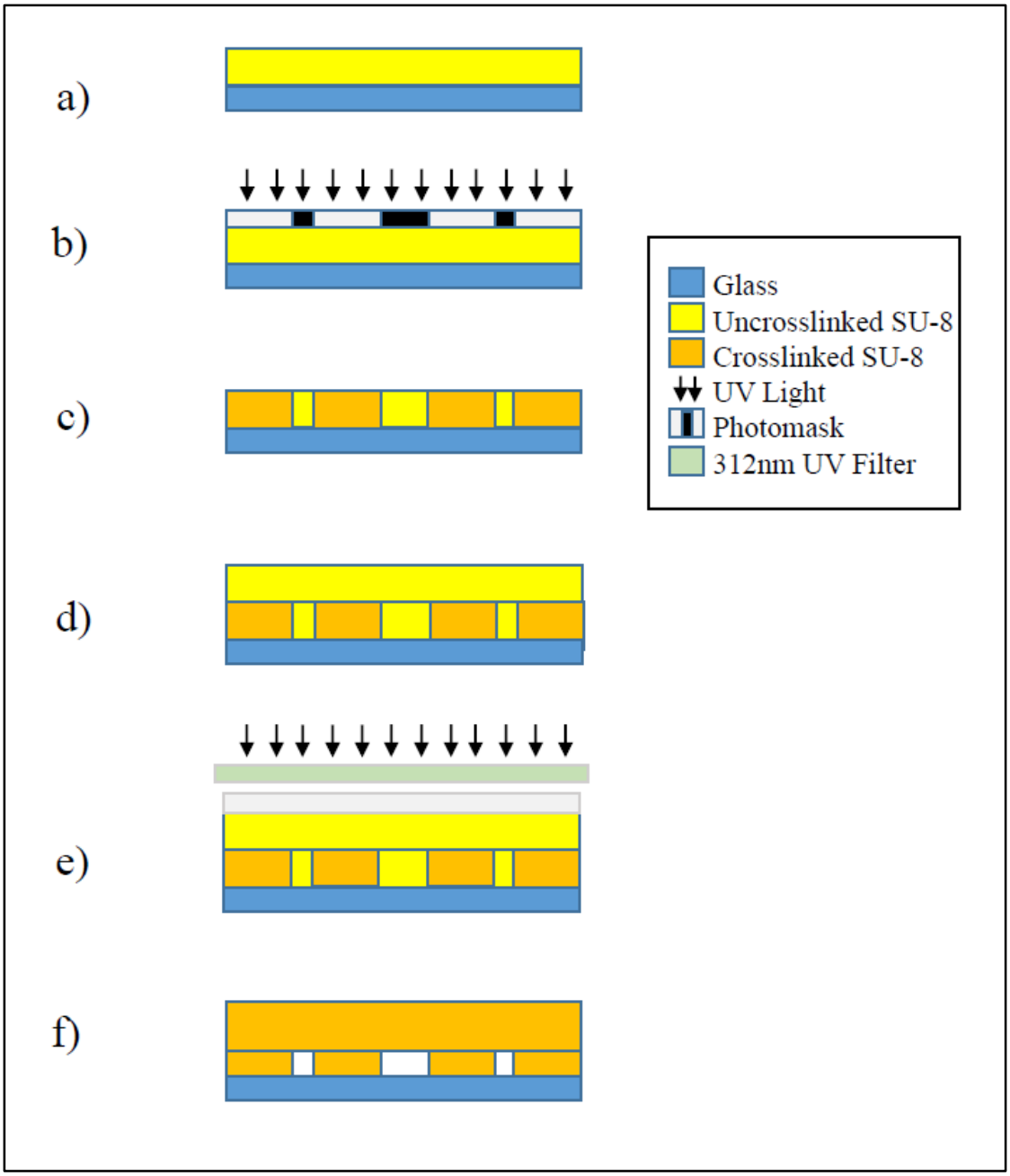

Figure 4.2: Process Flow for Partial Exposure Method: 2-Layer 2-Exposure. a) The SU-8 is first spin coated onto a clean glass substrate. b) The first layer is exposed with layer 1 mask without the UV filter. c) The resulting features are revealed after a PEB step. d) The second layer of SU-8 is spin coated on top of the exposed first layer. e) The second layer is patterned using a UV filter, aligning the features of layer 2 mask to match the layer 1 pattern with the use of a mask aligner. f) The final structure produced after development, which would create enclosed microchannels.

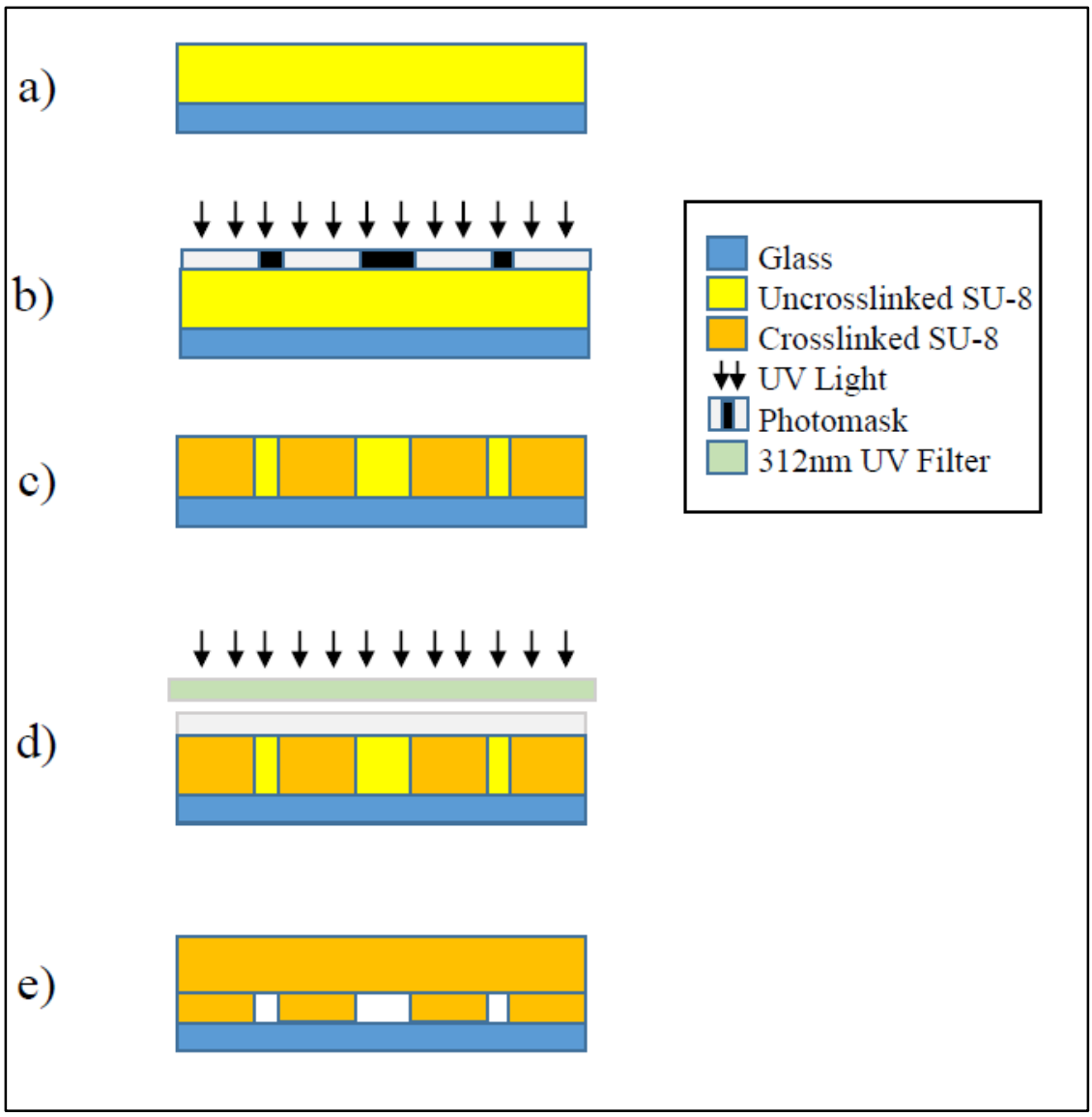

Figure 4.3: Process Flow for Partial Exposure Method: 1-Layer 2-Exposure. a) The SU-8 is first spin coated onto a clean glass substrate. b) The first layer is exposed with layer 1 mask without the UV filter. c) The resulting features are revealed after a PEB step. d) The features of layer 2 mask are aligned to the already exposed pattern of layer 1 using a mask aligner, and are exposed through the UV filter. e) The final structure produced after development, which would create enclosed microchannels.

4.3 Inverted Build Method

This protocol is modified from procedures by Tuomikoski and Blanco, which creates a pattern and a sealing layer on two different substrates that can be bonded together to create the enclosed microchannel [17], [18]. For these inverted build tests, the two layers of SU-8 are patterned in reverse order onto a silicon wafer while another blanket sealing layer is fabricated on glass. The features of mask 2 are patterned first on the silicon wafer, while the mask 1 design would be patterned on top in a separate layer of SU-8. The substrates are bonded together, and the silicon wafer is released to leave behind our desired SU-8 enclosed microchannels on a glass slide, essentially transferring the two-layer SU-8 structure from the silicon wafer to the glass slide. For this build scenario, we test two bonding procedures as well as two release protocols.

Both bonding methods begin with SU-8 being patterned onto a silicon wafer. The silicon is not cleaned using an HF dip, as we hope to later release the SU-8 from the wafer. Instead, the wafer undergoes a mild solvent rinse process using isopropanol, methanol, and acetone and the subsequent dehydration bake before spin coating of the first layer of SU-8. Since this would be built in reverse, a thick 50μm layer is patterned with the Layer 2 mask is processed first. The thin 10μm layer is coated on top, and exposed with the mask aligner. No filter is needed here, because the smaller features of Layer 1 would sit on top of the larger Layer 2 features. Overexposure of Layer 1 would not ruin the features of Layer 2, and it would improve adhesion of the top layer to the bottom one.

4.3.1 Unexposed Bonding

The first method for bonding involves an unexposed layer of SU-8. On a separate glass substrate, a thick 50μm layer is coated onto the slide. The glass substrate is heated to 65°C to begin the soft bake procedure. During the transition to the higher temperature at 95°C, the glass substrate gets clamped to the patterned SU-8 on the wafer to create the bond. After completing this soft bake process, the unexposed layer on the glass slide is then exposed through the backside of the glass. This step would crosslink the layer on the glass, and complete the bond to the SU-8 layers. If not exposed, the construct would fall apart when the SU-8 is developed. The process flow for the unexposed bonding method is shown below in Figure 4.4.

4.3.2 Exposed Bonding

Unlike the previous method, the layer of SU-8 on glass is fully exposed before it is bonded to the SU-8 layers on the wafer. This layer is blanket exposed to crosslink the entire layer to serve as a flat base that can adhere to the patterned features on the silicon wafer. The SU-8 on the glass is then clamped together to the SU-8 on the wafer and heated to 85°C for 20 minutes. Bonding is performed at this temperature, since it is just above the SU-8 glass transition temperature. The wafer is then released, and the undeveloped 2-layer pattern on the wafer is transferred to the glass. The SU-8 is then developed to reveal the enclosed microchannel. The process flow is shown below in Figure 4.5.

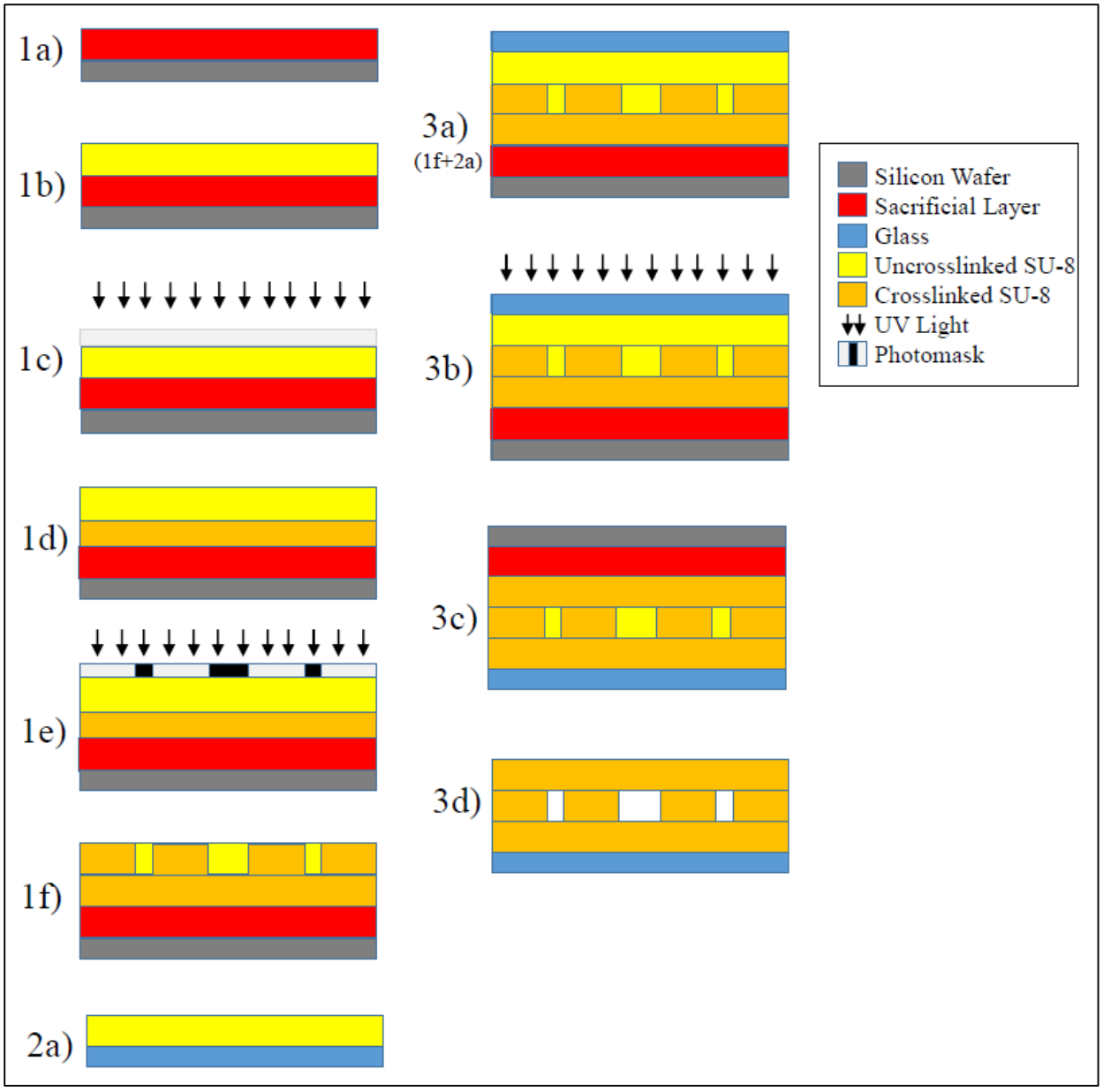

Figure 4.4: Process Flow for Inverted Build Method: Unexposed Bonding. 1a) A layer of sacrificial material is first spin coated onto a silicon wafer. 1b) A layer of SU-8 is then coated on top of the sacrificial layer. 1c) The first layer of SU-8 is patterned with layer 2 mask before undergoing PEB. 1d) The second layer of SU-8 is spin coated on top of the patterned first layer. 1e) The second layer is exposed with layer 1 mask. 1f) The resulting SU-8 structures are created on a silicon wafer. 2a) A layer of SU-8 is spin coated onto a clean glass surface. 3a) The completed SU-8 structures patterned on the silicon wafer are bonded with the single layer of unexposed SU-8 on the glass slide. 3b) The unexposed layer of SU-8 is exposed through the backside of the glass while on top of the silicon wafer construct. 3c) The sacrificial material is removed to release the silicon wafer. 3d) The SU-8 layers on the glass substrate are developed to reveal enclosed microchannels.

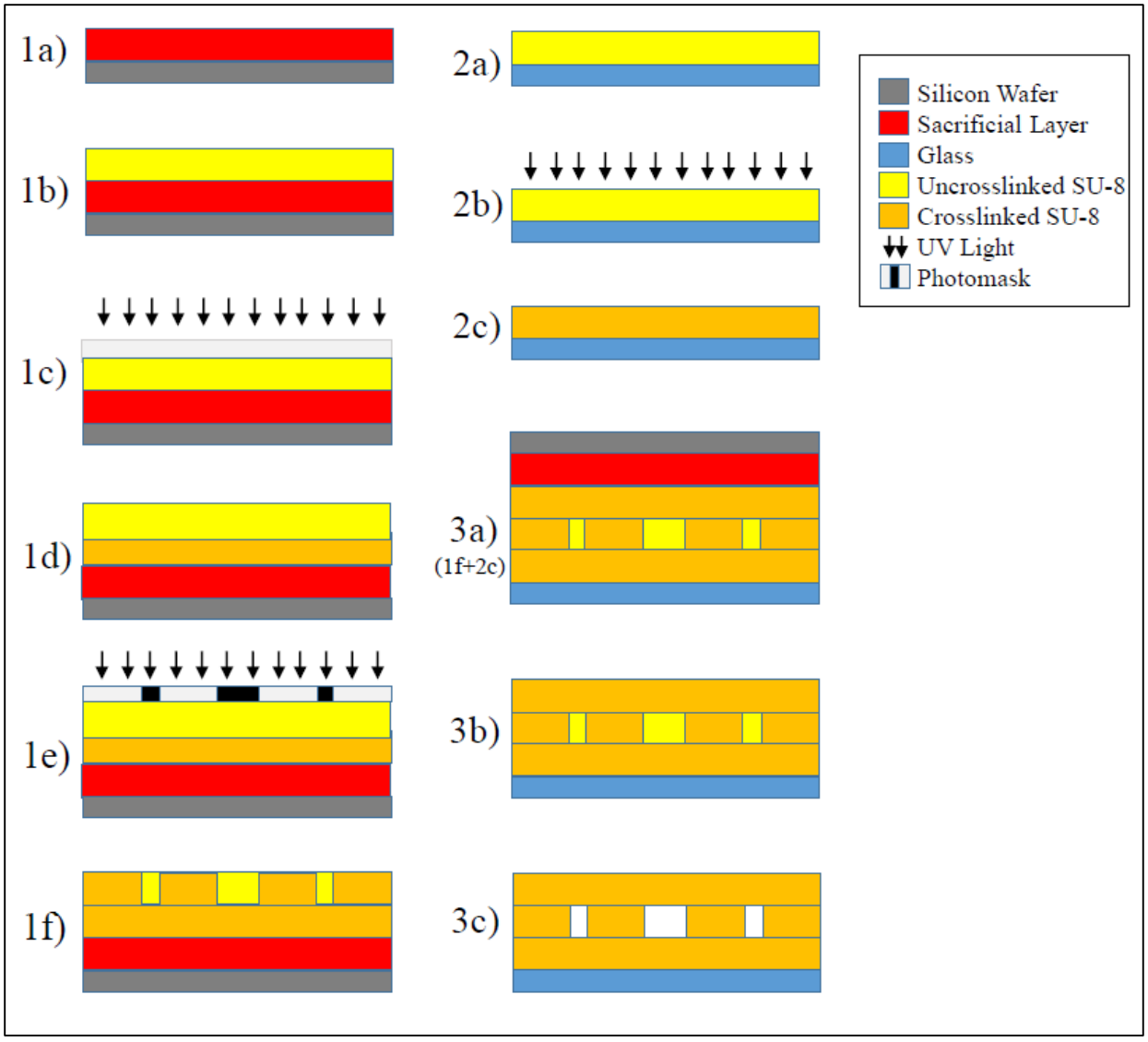

Figure 4.5: Process Flow for Inverted Build Method: Exposed Bonding. 1a) A layer of sacrificial material is first spin coated onto a silicon wafer. 1b) A layer of SU-8 is then coated on top of the sacrificial layer. 1c) The first layer of SU-8 is patterned with layer 2 mask before undergoing PEB. 1d) The second layer of SU-8 is spin coated on top of the patterned first layer. 1e) The second layer is exposed with layer 1 mask. 1f) The resulting SU-8 structures are created on a silicon wafer. 2a) A layer of SU-8 is spin coated onto a clean glass surface. 2b) The SU-8 layer is completely exposed without pattern. 2c) The complete blanket layer of SU-8 is fabricated onto a glass surface. 3a) The completed SU-8 structures patterned on the silicon wafer are bonded with the single layer of SU-8 on the glass slide. 3b) The sacrificial material is removed to release the silicon wafer. 3c) The SU-8 layers on the glass substrate are developed to reveal enclosed microchannels.

4.3.3 Release Tests

We use a layer of sacrificial material that is coated on the wafer before the processing of the SU-8 structure. This layer is removed to release the wafer from the SU-8 features. We explore the use of positive photoresist SC1827 that dissolves in developer solution or silicon dioxide that can be etched using HF, as previously described in Section 4.1.

The first possible sacrificial material is positive photoresist SC1827. One benefit of using positive photoresist is that it is simple to coat onto the wafer substrate, and it can easily be removed using MF319 developer solution. The SC1827 would be partially exposed during the patterning of the transparent SU-8 layers, but both exposed and unexposed SC1827 is also soluble in the SU-8 developer solution. This has its benefits, as the sacrificial layer is removed in the same step as the development of the SU-8 patterns. Unfortunately, this would not allow for the development of the patterns before bonding, which could alter the features and possibly close off the intended microchannel spaces.

Another release mechanism is to use a Buffered Oxide Etch procedure to etch the silicon dioxide on the wafer to release the SU-8 layers. By skipping the HF dip normally used to clean wafers, we retain the native silicon dioxide layer on the silicon surface to be sacrificed later on to release the wafer. As mentioned earlier, BOE is a more dangerous process that would also etch glass, so this method must be timed properly to only remove the silicon dioxide layer while maintaining the structure of the support glass. However, if the glass slide must be sacrificed, a thicker blanket layer can be created on glass to serve as the base of the SU-8 microchannel construct.

For each combination of bonding and release methods for this inverted build test, the SU-8 is developed after bonding has occurred. Blanco and Tuomikoski bond fully developed

layers of SU-8 together to form their microchannels, but this is not suitable for our experiments with our options of sacrificial materials [17], [18]. If using positive photoresist, the SU-8 developer would begin to release the wafer before the patterns have bonded to the secondary substrate. If using BOE to release the wafer, residual BOE solution and the dangerous HF component may remain in the spaces of the formed microchannel.

4.4 Chapter Summary

Each fabrication process must begin with proper preparation of the substrate. Typically, a silicon wafer is dipped in hydrofluoric acid to remove the silicon dioxide layer, which would improve SU-8 adhesion to the hydrophobic silicon substrate. Glass is cleaned using a RCA-1 solution or a piranha solution, both of which are used to remove debris and other contaminants that would interfere with photoresist processing.

The first proposed process, modified from a procedure from Ceyssens, is a partial exposure method using a UV filter to limit wavelengths directly fabricated onto a glass substrate. The UV filter must first be characterized to determine appropriate exposure energies to achieve certain depths. We initially attempt a 2-layer 2-exposure method, where the first layer is patterned normally with Layer 1 mask and a second layer is created and patterned with Layer 2 mask through the UV filter. A modified approach uses a 1-layer 2-exposure method, where a single thicker layer is first patterned with Layer 1 mask, and Layer 2 mask is then exposed through the UV filter. This method would directly create SU-8 features onto a glass substrate for the final platform.

An alternative inverted build method is based off of procedures from Blanco and Tuomikoski. In these methods, the patterns are fabricated on a silicon wafer in reverse order,

and the two-layer SU-8 patterns are transferred to a glass substrate through an exposed or unexposed bonding step and release step. For an exposed bonding step, an unpatterned layer of SU-8 is fully exposed on a glass slide and is then brought in contact with the patterns on the wafer and heated above the SU-8 glass transition temperature. In unexposed bonding, the SU-8 layer on glass is bonded to the other layers during the soft bake process, and it is then exposed through the backside after bonding is completed. Releasing the wafer after bonding requires a sacrificial material on the silicon wafer before processing of the SU-8 layers. The wafer can be coated with positive photoresist SC1827, which would dissolve in SU-8 developer solution during the same step as SU-8 pattern development. Another option to release the wafer would be to use native silicon dioxide as a sacrificial layer, which can be removed using HF after bonding is complete. This method requires the use of a handle wafer as a means of transferring the patterns onto our desired glass substrate.

CHAPTER 5

Results and Discussion

5.1 Introduction

The goal of the project is to successfully fabricate a device for the study of tunneling nanotubes. We varied the cleaning procedures and tested different possible build protocols to create an optically clear platform. Each process using negative photoresist SU-8 is performed in sequential order, so successful completion of the device can only be evaluated after final development step. The most basic measure for success would be to have the microscale SU-8 features remain on the surface of the glass without any delamination, or peeling. Many test results do not include pictures, since SU-8 often completely delaminated from the surface to leave behind the glass slide substrate.

For some preliminary tests, we chose to use larger patterns for better visibility, since it would be more obvious if these features delaminated from the substrate. Since the mask designs for Layer 1 and Layer 2 have fine features, it is unlikely that small patterns would remain on the surface if larger ones did not. Common features we tested include a 2mm square block pattern and a spiral channel of 500μm width.

5.2 Partial Exposure Method

Initial testing begins with the intention of using a 10μm layer of SU-8 3005 for Layer 1, followed by a 50μm layer of SU-8 2050 for the second patterned layer exposed through a UV filter as part of a 2-Layer 2-Exposure technique. For the partial exposure method, we first

need to characterize the filter for SU-8 2050 so that we can achieve the proper exposure energy necessary to expose only the top layer without reaching the bottom one.

5.2.1 UV Filter Characterization

We first spin a 50µm layer of SU-8 2050 on the surface, and exposure is done through the backside of the glass testing a range of energies. The process is described in Section 4.2, with SU-8 layer processing as described in Table 2.2. To fully expose a 50µm layer of SU-8 2050 requires 240 mJ/cm^2 of exposure energy, based on a suggested 160 mJ/cm^2 value with a 1.5x multiplier for a glass substrate [14]. Using a UV intensity meter, we measured that the filter attenuates the lamp power to approximately 15%. We wanted to test a range of dosages that would allow for 240 mJ/cm^2 to reach the surface through the filter. Table 5.1 below shows exposure energies and the corresponding measured heights.

Exposure Energy from UV Lamp (mJ/cm^2)	Estimated Exposure Energy through Filter (mJ/cm^2)	Measured Height (µm)
240	(no filter control)	50
2040	320	48
1910	300	47
1530	240	48
1275	200	47
1020	160	47
765	120	--
600	95	--
510	80	--

Table 5.1: Exposure Energy Test Range and Results. This table shows the exposure energy values and the estimated energy that would reach the surface of the SU-8 through the filter. The last column shows the profilometer measurements, however the lowest dosages were not properly exposed, and an accurate measurement could not be made.

As a result of these exposure energy tests, we can see that there is very little difference in profilometer surface readings. However, with lower energy exposures, the SU-8 surface appears crackly and cloudy, as opposed to the clear solid surface of the properly exposed areas. A profilometer reading is not accurate, since the surface is not smooth enough to find a comparable baseline to measure. Pictured below in Figure 5.1 is a sample of one of the characterization tests.

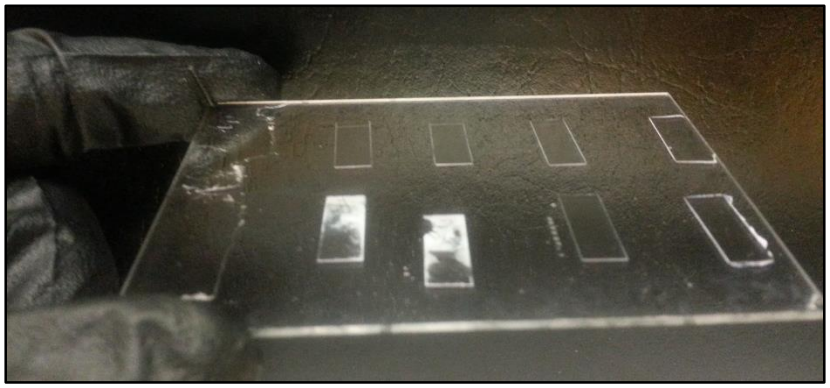

Figure 5.1: UV Filter Characterization Test Slide. For the ten positions, there are two control positions along with eight test sites. The two cloudy samples represent the lowest energy levels that were not fully exposed, while the other six sites are fully exposed. The two test samples on the far left were not processed correctly and were unmeasurable.

Another main observation with these tests is frequent delamination of the SU-8 from the glass. While the sample is submerged in developer solution to remove the unexposed regions, some patterned portions also begin to peel off from the surface of the glass, especially near the edges of the glass slide.

5.2.2 Experiment: 2-Layer 2-Exposure

From the filter characterization, we moved to a 2-Layer approach with a 10μm layer of SU-8 3005 followed by the 50μm layer of SU-8 2050. The 10μm layer of SU-8 3005 is

processed according to Table 2.2. For one sample, the entire surface is exposed without any patterns, while a parallel experiment is patterned with a spiral design. After a PEB step for these samples, they are coated with the following thick 50μm layer of SU-8 2050. Test samples are exposed with a block pattern through the filter at 1530 mJ/cm^2 and 1910 mJ/cm^2, which corresponds to 240 mJ/cm^2 and 300 mJ/cm^2 reaching the surface of the 50μm layer. With the non-patterned 10μm layer, we noticed delamination of SU-8 3005 from the glass. For the patterned sample, test sites were both overexposed on the top layer, resulting in features ruined in the bottom layer. The areas of the spiral pattern on the 10μm layer not covered by the block also delaminated from the glass slide.

We also tried using the newer formulation of SU-8 3050 to create a 50μm layer. We expected that the 3000 series would adhere better to itself and the glass substrate. The 10μm layer of SU-8 3005 is processed normally and blanket exposed without a pattern. During the soft bake of the 50μm layer of SU-8 3050, the layer seemed to have retracted and hardened in the center of the area of the slide, as shown below in Figure 5.2. This may be a result of uneven heating or too drastic of a temperature change in a short time period.

Figure 5.2: SU-8 3050 on SU-8 3005. The top slide shows an uneven layer of SU-8 3050 on top of 10μm layer of SU-8 3005. The bottom slide is a single 10μm layer of SU-8 3005.

The next test also used other SU-8 formulations, combining a 4μm layer of SU-8 2 with a 50μm layer of SU-8 2050. The 4μm layer of SU-8 2 is processed according to Table 2.2, and patterned with a spiral design. The 50μm layer of SU-8 2050 is processed normally and exposed with a block pattern using three test dosages through a filter and a non-filtered control. For this set of exposures, the glass slide is placed on top of a silicon wafer, which would reflect the UV light so a 1.5x factor for a glass substrate is not necessary, and the non-filtered control requires a recommended 160 mJ/cm^2 exposure energy [14]. We tested 160 mJ/cm^2, 240 mJ/cm^2, and 320 mJ/cm^2 for exposure through the filter. Only the control and the 320 mJ/cm^2 filtered exposure retained the features, while the other two test sites of SU-8 2050 delaminated during development. However, there was still noticeable delamination of the spiral features of the 4μm layer of SU-8 2 in areas not covered with the block pattern of SU-8 2050.

As a result of these 2-layer SU-8 experiments, we noticed continued delamination of SU-8 from glass and between the two layers of SU-8. We attempt to modify the surface of the glass through various surface treatments, which include a HMDS surface prime, a BOE treatment, a coating layer of silicon, and additional adhesion layers of SU-8. At the same time, we also considered switching from a 2-Layer 2-Exposure approach to a 1-Layer 2-Exposure method to reduce the number of SU-8 layers that could delaminate from each other. We continued to test a 2-layer method with the surface treatments, as well as the new 1-layer approach with modified substrates.

5.2.3 Substrate Surface Treatment

A shear analysis of SU-8 3000 on glass shows that it can withstand 23 MPa, while SU-8 2000 has poor adhesion [23]. As the project developed, we tried to modify the substrate surface in a number of ways. All glass had already been cleaned using RCA-1 or piranha before possibly undergoing further surface treatments. Some additional modifications include chemically priming the surface, etching the glass surface, or adding layers of SU-8 or silicon to improve adhesion of our SU-8 construct to glass.

The likelihood that SU-8 sticks to the glass surface depends on feature size and the thickness of the SU-8 layer. With larger features, there is more area in contact between the SU-8 feature and the glass slide to allow for better adhesion. The features in Layer 1 mask and Layer 2 mask have very small areas in each square of the grid, surrounded by large blanket spaces in between.

HMDS Surface Prime

As suggested by MicroChem to improved adhesion, the cleaned glass surface is primed with hexamethyldisilazane (HMDS). SU-8 3000 on glass primed with HMDS is able to withstand 44 MPa of shear stress [23]. This HMDS coating makes a surface more hydrophobic, allowing for better adhesion of SU-8. However, over-priming may lead to uneven coating of photoresist, resulting in bubbles that can cause defects in features. HMDS is a liquid that is applied to the substrate using a spin coater to distribute the solution. After a normal dehydration bake at 120°C for over 2 hours, HMDS is spun at 2000 rpm for 5 seconds. Excess solution evaporates at room temperature, but the slide is baked at 120°C for 10 minutes to ensure that the surface is dry [24].

For these experiments, a 60μm layer of SU-8 is spin coated onto the HMDS primed surfaces using SU-8 2050 or 3050. The upgraded SU-8 3050 should have better adhesion than SU-8 2050, so both SU-8 types are tested. The 60μm layers are prepared according to spin recipes listed in Table 2.2. The slides exposed with the overall mask design. The resulting slides are shown below in Figure 5.3.

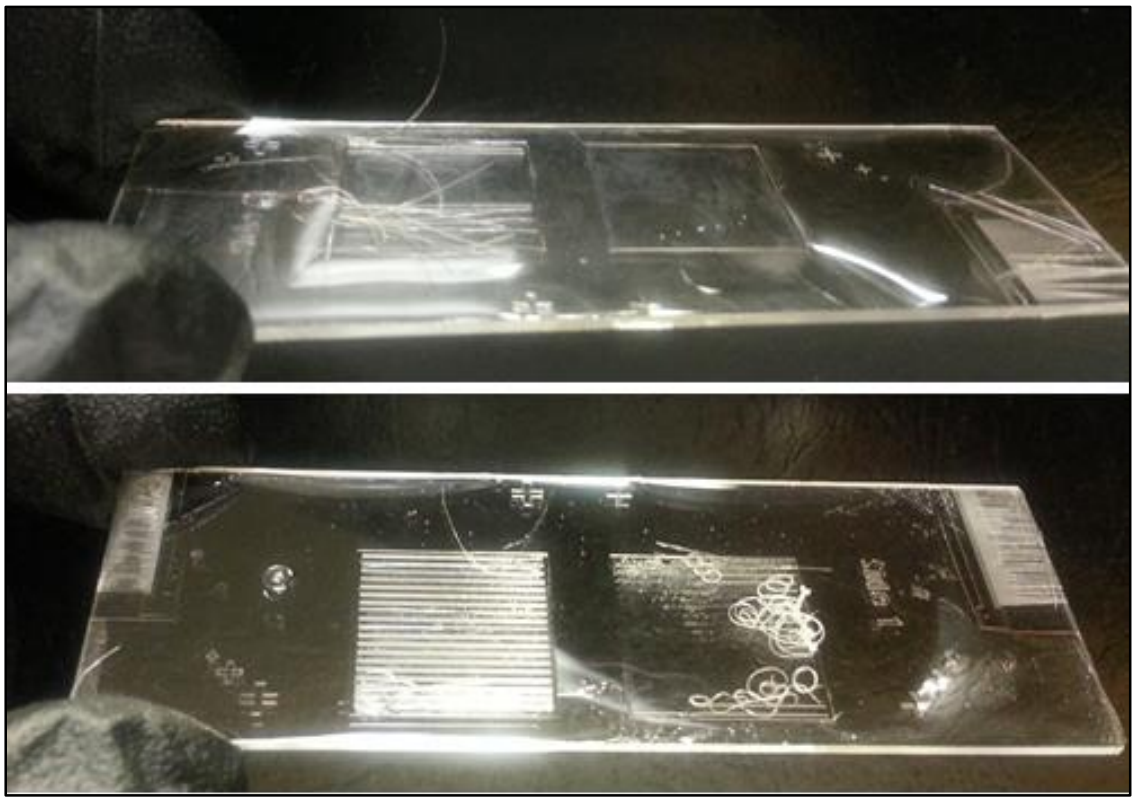

Figure 5.3: SU-8 Tests on HMDS-Primed Surfaces. (Top) A 60μm layer of SU-8 2050 on a HMDS primed surface shows more delamination of the features. (Bottom) A 60μm layer of SU-8 3050 on a HMDS primed surface. Although the bottom slide still shows delamination, there is noticeably better adhesion using SU-8 3050 than SU-8 2050.

Overall, the primed surfaces allowed for better SU-8 adhesion than non-primed surfaces, with SU-8 3050 showing to adhere better than SU-8 2050. As these designs have very fine features, many features still tend to delaminate from the glass while large blanket

areas remain on the surface. However, even these large areas of SU-8 still begin to delaminate at the edge of the glass.

According to other HMDS processing guidelines from Yield Engineering Systems, Inc., a vapor prime is more efficient in creating an HMDS monolayer than the liquid prime process [25]. The spin coating procedure may create a thicker layer of HMDS and could "overprime" the surface, causing pockets and "mousebites" in the photoresist features. The vapor prime procedures is combined with the dehydration bake process to removes moisture from the wafer and replace water molecules with HMDS to make the surface more hydrophobic. The vapor prime creates a larger contact angle than the spin coat liquid prime process, and maintains surface hydrophobicity for a longer period of time. The contact angle formed by water on the hydrophobic surface created from a liquid prime procedure begins to degrade after 3 days, while the vapor prime method is stable for at least two weeks [25].

The primed surface is used immediately, so the longer stability of the water contact angle does not play an important factor. Although the liquid primed substrates did improve adhesion, glass coated in HMDS via vapor prime could further improve SU-8 adhesion.

Buffered Oxide Etch Treatment

One surface modification was a Buffered Oxide Etch (BOE) which etches thin oxide films or polysilicate glass. We hoped that a brief etch time would roughen the surface of the glass and improve adhesion of subsequent SU-8 layers. Similar to the wet processes of HF dipping, RCA-1 and piranha cleaning, the BOE procedure also requires the use of extra protective gear in the form of nitrile gloves, a chemical apron, and a safety shield. The BOE solution is made from combining 20 ml of 49% HF with 80 g of powdered ammonium

fluoride (NH_4F) dissolved in 120 ml of DI water [26]. The BOE solution is maintained at room temperature and is poured into a polypropylene beaker. Since the amount of etch is dependent on exposure time, we varied the time for how long a glass slide is submerged within the solution. The used BOE solution is disposed in the proper waste containers. Figure 5.4 below shows glass that has been cleaned using piranha and glass that has undergone an additional 15 seconds of BOE treatment.

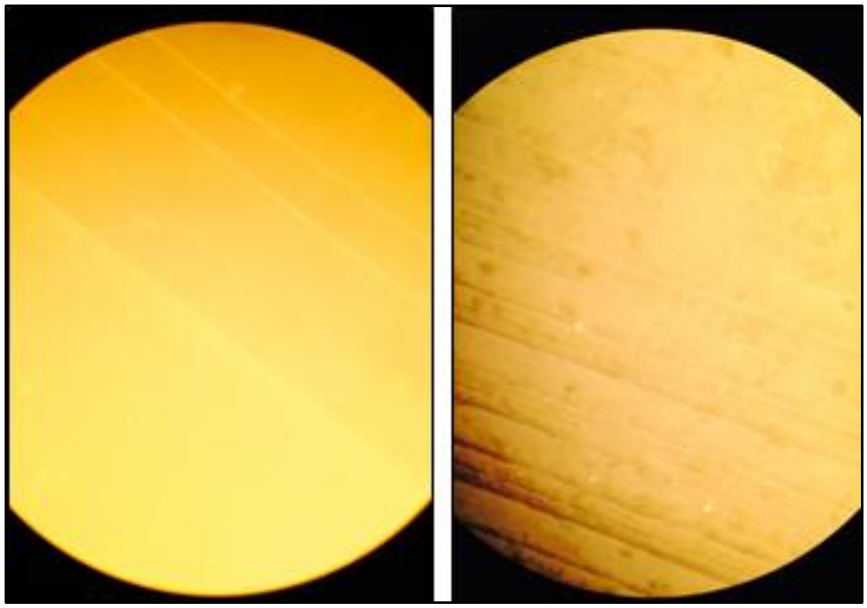

Figure 5.4: Microscope Images of Glass Slides with BOE Treatment. (Left) Glass slide cleaned with piranha solution. (Right) Glass slide with piranha solution, with an additional 15 seconds of treatment in a BOE solution.

We hoped the additional BOE treatment would create a rougher surface on the piranha-cleaned glass for improved SU-8 adhesion. We tested three etch times of 15 seconds, 30 seconds, and 45 seconds to see how longer etch times affected the glass substrate. To test adhesion, each glass substrate was coated with a 10μm layer of SU-8 3005 and exposed with the square block and spiral pattern.

Glass slides etched with BOE for 30 seconds and 45 seconds did not retain any SU-8 features, including the large block feature. The 15 seconds of etch was the most promising of the three BOE samples, but it did not seem to have much difference than the original piranha-cleaned glass. Although we had hoped the rougher surface would allow for more adhesion sites for the SU-8, the BOE samples seemed to have a negative effect and promoted more delamination instead of adhesion.

Silicon Coating

SU-8 adheres better to a silicon substrate, with SU-8 3000 able to withstand 71 MPa and SU-8 2000 able to withstand 53 MPa of shear stress. Therefore, we attempted to apply a thin layer of silicon coating on the glass to improve adhesion of SU-8. Using an e-beam evaporator, 100 Angstroms of silicon is deposited onto the glass. The thin silicon coating gives the glass a slight yellow tint that is still transparent, as shown in Figure 5.5.

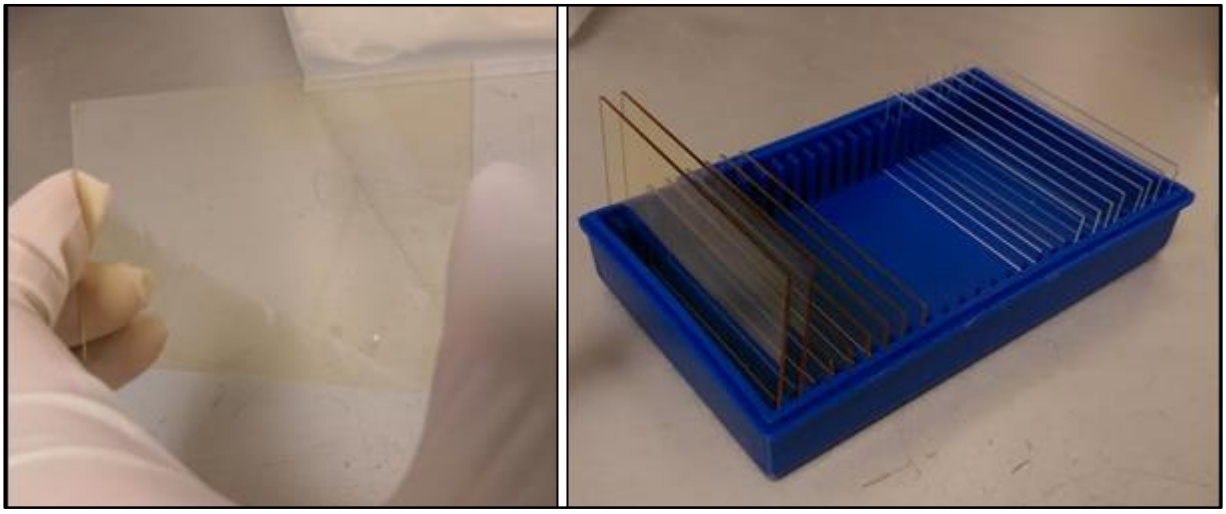

Figure 5.5: Silicon-Coated Glass Slides. (Left) A silicon coating provides a slight yellow tint to the slide. (Right) Silicon-coated glass slides in a slide box are clearly different when compared to normal piranha-cleaned glass slides.

We hoped that a thin layer would be enough to improve adhesion of the SU-8 construct. For some silicon-coated glass substrates, we also wanted to include metal alignment marks for better visualization. Alignment marks are fabricated according to the procedure outlined earlier in Section 2.2 using positive photoresist.

One main concern from this surface modification is still the visibility, since this coated layer is not optically clear. However, a 100 Angstrom layer is thin enough to fulfill our visual requirement that will allow cells to be seen using an upright microscope. A 50 μm layer of SU-8 is coated onto the silicon surface and exposed with Layer 1 mask. Although there was some slight improvement in SU-8 adhesion, the thin features of our mask still delaminated from the substrate, as shown below in Figure 5.6.

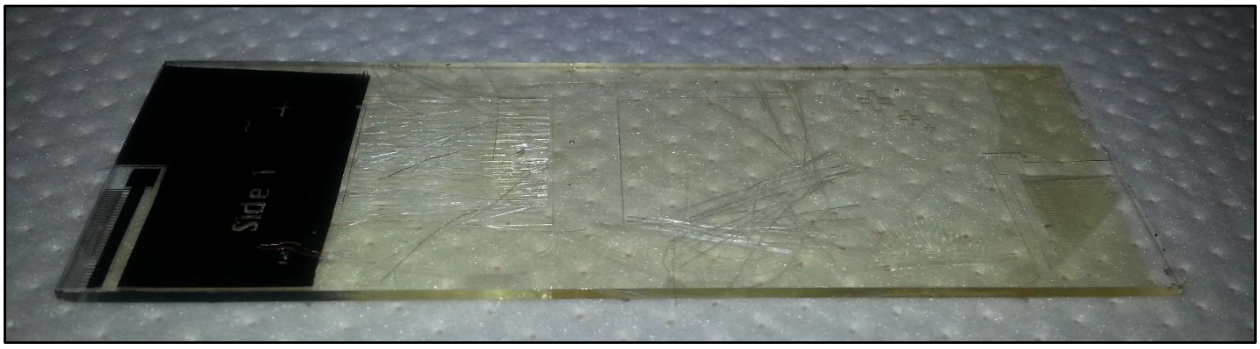

Figure 5.6. SU-8 on Silicon-Coated Glass with Metal Alignment Marks. The slight yellow tint of the silicon can be seen, with the metal alignment marks on the left side of the slide. The thin SU-8 features still delaminated from the surface of the slide.

SU-8 Adhesion Layer

In addition to using SU-8 as the structure material, we also used SU-8 as an adhesion layer. Because SU-8 already has multilayer capabilities, it should adhere well to itself. We tried both thin and thick unpatterned blanket layers in between the glass substrate and our patterned layers. With different SU-8 types capable of achieving the same thickness, we

varied between using the original SU-8, the SU-8 2000 series, and the SU-8 3000 series. Briefly, the procedure for creating these adhesion layers is to spin coat the SU-8 onto the glass substrate, soft bake, and expose without any patterns, followed by a post-exposure bake process.

In continued testing of the 2-Layer 2-Exposure method, these adhesion layers would create a 3-layer experimentation. For the 1-Layer 2-Exposure method, we would then achieve the 2-layer experiments we had already previously done.

For thin adhesion layers, we attempted a 5μm or 10μm layer of SU-8 3005, and 2μm layer of SU-8 2002. These layers are prepared according to the spin recipes in Table 2.2. Because of SU-8 3000 series having better adhesion to glass, we hoped that the 5μm or 10μm layer of SU-8 3005 would be the best option. However, after processing of the blanket adhesion layer, the following spin coating of the 10μm layer of SU-8 3005 did not coat evenly, as shown below in Figure 5.7. This is most likely a result of incompatibility of the surface chemistry of the two thin layers.

Figure 5.7: SU-8 3005 on SU-8 3005. After complete processing of the first 10μm layer of SU-8 3005, the second layer of SU-8 3005 did not evenly disperse during spin coating.

As part of a 3-layer test, we used a 2μm layer of SU-8 2002 as an adhesion layer followed by a 10μm layer of SU-8 3005 patterned with spirals. The third layer is a 50μm layer of SU-8 2050 exposed through a filter with a block pattern testing dosages of 420 mJ/cm^2, 480 mJ/cm^2, 540 mJ/cm^2, and 600 mJ/cm^2. A test sample with the first two layers appeared to be processed well, but still featured some delamination at the edges. For a sample with all three layers, the 50μm layer delaminated completely for every exposure. This might be as a result of underexposure through the filter.

Since thin adhesion layers were not helpful in retaining features of the patterned layers, we turned to creating a thicker adhesion layer. We attempted a thick 120μm layer of SU-8 2050, followed by a thin 2.9μm layer of SU-8 2002, and a 50μm layer of SU-8 2050. These layers are prepared according to the spin recipes in Table 2.2. With our initial experiments, we noticed wrinkling in the surface during the soft bake process of the thick adhesion layer. This is most likely caused by uneven heating, where the solvent dries from the surface faster than the inside of the thick layer. As a result, the subsequent thin layer may not have spin coated evenly. After the pattern is exposed in the thin layer, we continued to spin the thick 50μm layer and expose the second pattern. In development, we noticed complete delamination of the two patterned layers, leaving behind the wrinkled thick blanket layer on the glass. With a thick blanket layer, the subsequent 10μm layer of SU-8 3005 was successfully spin coated evenly and processed on top. However, later development steps still showed delamination of the patterned features.

5.2.4 Experiment: 1-Layer 2-Exposure

For this procedure, we moved to spinning a thick 60μm layer of SU-8 2050, following the processing steps in Table 2.2. The first test sample is first patterned with a spiral channel. The second exposure requires the use of a filter with an energy dosage of 600 mJ/cm^2. Although this value was on the lower range based on the UV filter characterization tests, the results of this experiment were consistent with previous 2-Layer 2-Exposure experiments showing that this energy level might still be too high.

This set of parameters was also tested using the actual Layer 1 and Layer 2 mask. The first exposure using Layer 1 mask is processed normally. After a PEB step, the features are more visible, allowing for Layer 2 patterns to be properly placed using a mask aligner. The experiment also resulted with an overexposure, and Layer 2 features encroached into the gap spaces of Layer 1 pattern. This can be attributed to an overpowered exposure energy, since the glass slide must first be mounted onto a silicon wafer to use the mask aligner. Since the silicon wafer reflects the wavelengths, the 1.5x factor for glass is not necessary in the suggested exposure energy to crosslink a 60μm layer of SU-8 2050.

5.2.5 Partial Exposure Method: Summary

Experiments using the UV filter were not consistent, and we were not able to properly tune our exposure energy to achieve a 50μm layer of SU-8 2050 that would not expose lower layers of SU-8. Even without the filter, we noticed delamination in many of these experiments, especially from the patterned layers. However, often times, many of the large blanket layers intended for adhesion began to peel at the edges of the substrate as well. Although we tried a variety of ways to improve adhesion of the SU-8 to the glass with HMDS

surface priming, silicon coating, and additional SU-8 adhesion coating, none of these methods worked for direct fabrication of the construct onto the glass surface. We then move on to our next attempt of fabrication procedure of an inverted build test.

5.3 Inverted Build Method

For a basis of fabrication, a single 50μm layer of SU-8 2050 is coated onto a HF-dipped silicon wafer and exposed with the mask according to the recipe in Table 2.2. Following a post exposure bake, a 10μm layer of SU-8 3005 is processed on top, and the mask is reversed and properly aligned for exposure. As a result of the mask design, half of the wafer has the long stripes of Layer 2 pattern on top of the small blocks of Layer 1 pattern, while the other half is inverted. As shown below in Figure 5.8, we see Layer 1 blocks with the 0.5 μm gaps on top of the long lines of the Layer 2 pattern with widths of 1, 3, 5, and 7 μm.

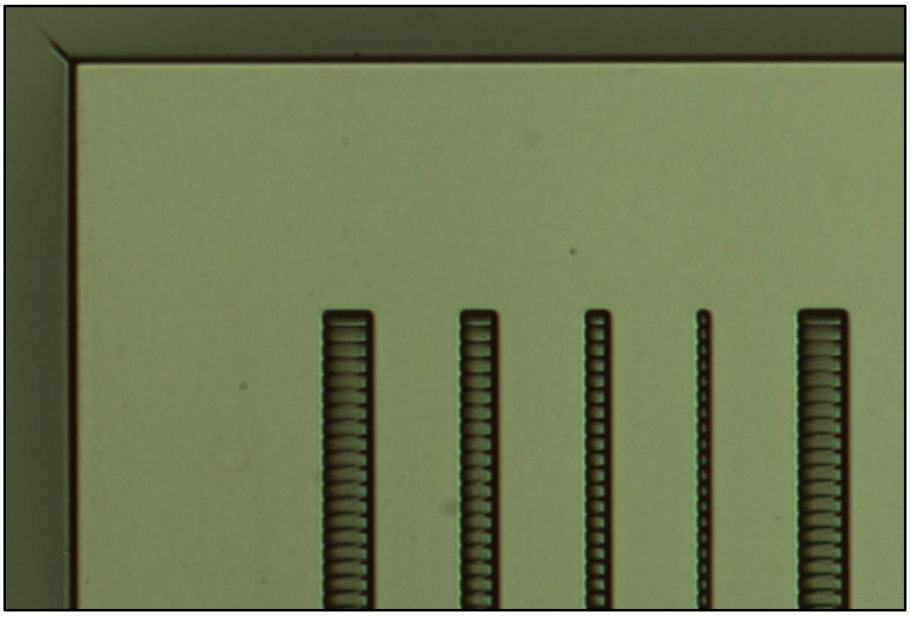

Figure 5.8: Microscope Image of 2-Layer Patterned SU-8 on a Silicon Wafer. At 2x zoom, we can see the individual blocks of Layer 1 positioned on top of the Layer 2 features.

5.3.1 Unexposed Bonding

For the bonding tests, the silicon wafer undergoes a dehydration bake, but it is not subjected to a HF dip so that the silicon dioxide layer remains intact for a release mechanism later. Since this is intended to test bonding, we only apply a single 50µm layer of SU-8 2050, which is patterned with our overall mask design and is processed to the PEB step. For the glass substrate, we used a larger 2in x 3in glass slide coated with a 50µm layer of SU-8 2050. The bonding process is described according to Figure 4.4. The SU-8 on glass is placed on the silicon wafer during the soft bake process on a 95°C hot plate, as shown below in Figure 5.9.

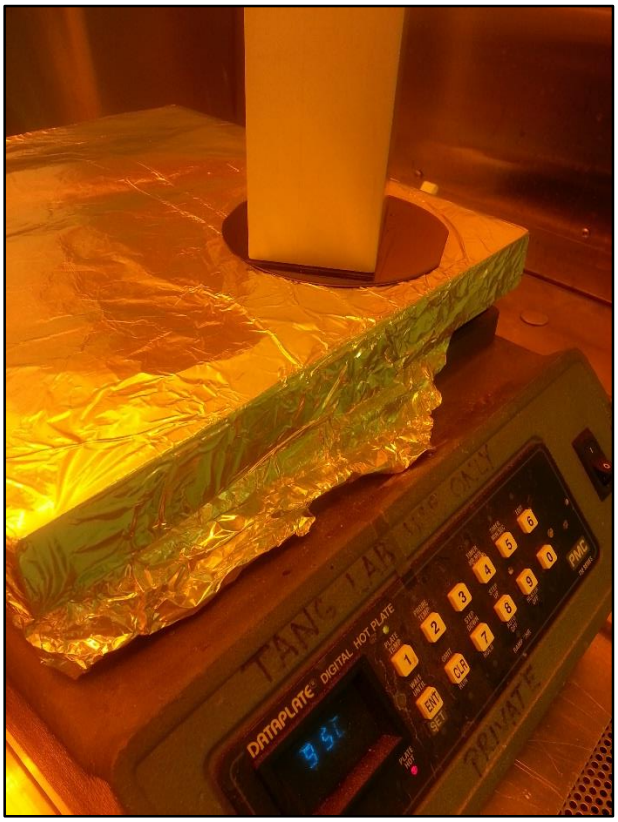

Figure 5.9: Unexposed Bonding Process. A weight applies pressure to the glass slide as it is positioned on the silicon wafer substrate, already patterned with a single layer of SU-8. This is maintained for the 7 minutes specified for the soft bake process of a 50µm layer of SU-8 2050, according to Table 2.2.

After the weight is removed, we can see that the glass slide had repositioned during the bonding step, since the SU-8 had not completely hardened when it is first placed together, as shown below in Figure 5.10.

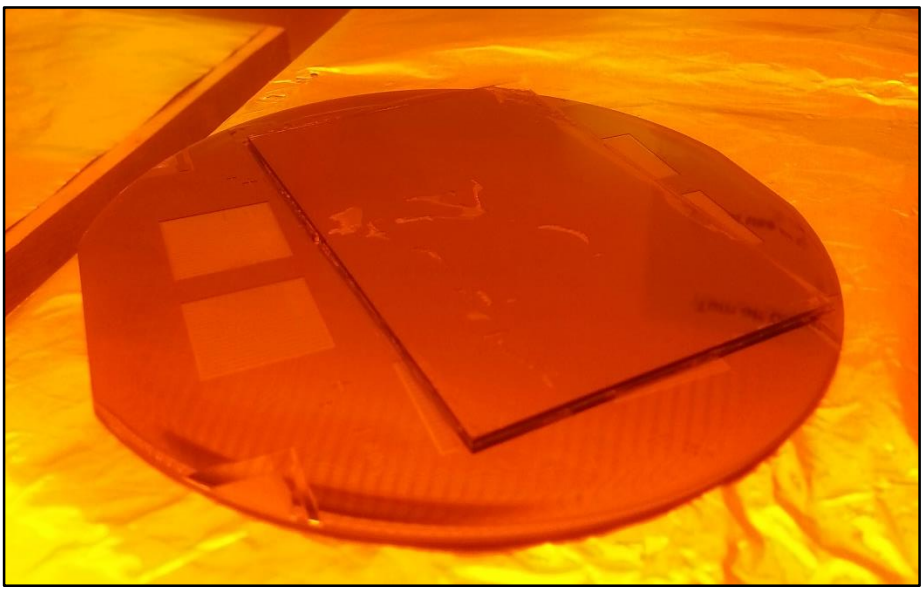

Figure 5.10: Misaligned Glass from Unexposed Bonding Process. The glass slide had been aligned onto the silicon wafer to cover the center features under the weight. The glass slide has moved from the original position due to the non-solid state of the SU-8 during the bonding process performed simultaneously with the soft bake.

Despite misalignment, when the construct is brought to room temperature and can continued to be processed. Even though the SU-8 layer is on a glass substrate, the silicon wafer is still intact and will reflect the UV rays, so the layer is blanket exposed through the backside of the glass with the recommended 160 mJ/cm^2. To protect the rest of the silicon wafer pattern from accidental exposure, the area around the glass slide is covered with aluminum foil. As usual, the newly exposed layer needs to undergo a PEB step. The entire construct is then submerged in the SU-8 developer solution to complete processing of all the SU-8 layers.

We can see that the patterns on the wafer are developed, but features are not visible under the glass slide. Most likely, the previously unexposed areas of SU-8 on the wafer have been exposed as part of the bonding step. Although the glass slide remained bonded to the silicon wafer, the SU-8 features were ruined in the process.

5.3.2 Exposed Bonding

In this procedure, the silicon wafer is processed in the same way as the previous unexposed bonding test using only a dehydration bake process. Again, a single layer of 50µm of SU-8 2050 is patterned with the final mask design, processed up to the PEB step. For glass slides, we coated two 1in x 3in glass slides with the same layer of 50µm of SU-8 2050. These slides are blanket exposed an undergo PEB to complete processing of the layer. As all layers of SU-8 have already been exposed, the two surfaces are brought together and heated to 85°C for 20 minutes, as described earlier in Figure 4.5. The surfaces are clamped together to apply pressure, as shown below in Figure 5.11.

Figure 5.11: Exposed Bonding Process. Glass slides are clamped onto wafer, and an additional weight is placed on top afterwards to add pressure to bond the layers of SU-8 together.

After the 20 minutes, the weight and clamps are removed. Some areas of SU-8 have melted together. Even before development, it is clear that these features would be ruined because of the uneven distribution of the bond. While the construct is submerged in SU-8 developer, the uncovered areas of the wafer show well developed features. However, the glass slides are not completely bonded, and can easily be removed from the wafer when the liquid developer gets in between the layers. The SU-8 features were also ruined as a result of the detachment of the glass. Figure 5.12 below shows the construct before and after development.

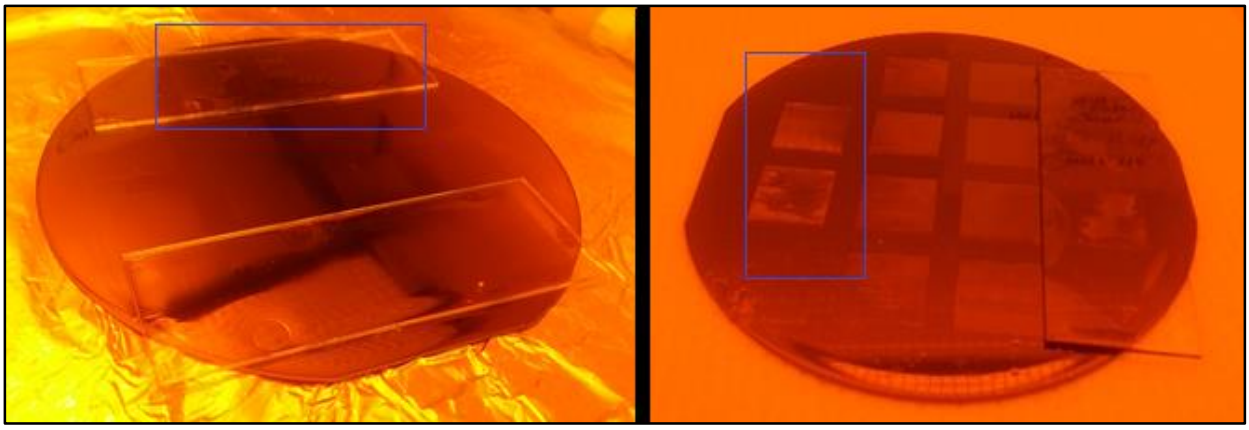

Figure 5.12: Development of Exposed Bonding Experiment. (Left) Before the construct is developed, areas of contact between the slide and wafer are noticeably unevenly bonded, as shown in the box. (Right) After development, the glass slide did not stay bonded, peeling away some of the features on the wafer in the same area.

Because the layers of SU-8 are already exposed, there's no risk of accidental exposure that is present with the unexposed bonding method. However, the bond created here is not as strong, since the glass slide becomes detached with the introduction of the SU-8 developer solution.

5.3.3 Release Tests

During the experiments to test bonding, we simultaneously prepare for possible release mechanisms, since the sacrificial layer material must be included on the wafer before any SU-8 processing can occur. As mentioned earlier to test both the exposed and unexposed bonding methods, we prepared the slides with the intention of releasing the wafers using a HF solution. Since neither bonding process appeared to be successful in our tests, continuing to attempt a wafer release using a HF solution is an unnecessarily dangerous procedure.

One issue is the inconsistency of the fabrication process. For one set of experiments, we prepared two wafers with only a dehydration bake process, and patterned the mask design on a single 50μm layer of SU-8 2050. When both of these wafers are developed in the SU-8 developer solution, one wafer appears to be properly processed, while the other wafer has delamination of the features, as shown below in Figure 5.13.

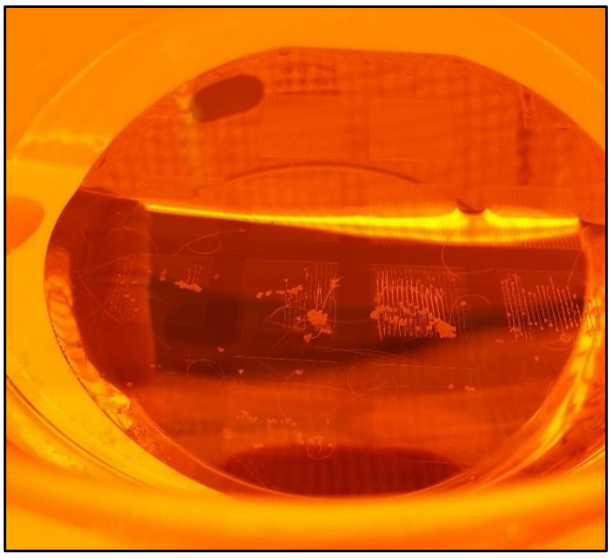

Figure 5.13: Delamination of SU-8 on Silicon Wafer. While still submerged in SU-8 developer solution, features begin to delaminate from the surface. Without the HF dip process, the silicon wafer has hydrophilic properties that do not allow for proper adhesion of SU-8.

This delamination is a result of the silicon dioxide layer that we had not removed with a HF dip. The hydrophilic nature of the surface did not allow for the SU-8 to adhere well to the surface, so the thin features began to peel away from the surface. The wafers utilized in the bonding tests did not require any extra processing steps, since the wafer only needs to undergo a dehydration bake to prepare for the next layer, unlike the use of positive photoresist SC1827.

To use of SC1827 as a sacrificial layer, the liquid photoresist is spin coated onto a wafer and processed according to the steps described earlier in Section 2.2. The layer can be blanket exposed that would help remove the material later, but this is an unnecessary since unexposed SC1827 is also soluble in SU-8 developer solution. A 50μm layer of SU-8 2050 is spin coated on top, and patterned with the mask design. When the SU-8 layer is developed, the square areas featuring the Layer 1 and Layer 2 features completely delaminate. The large exposed regions in between these squares remained on the surface of the wafer, even with the layer of SC1827 below it.

5.3.4 Inverted Build Method: Summary

The unexposed method was more efficient at bonding, but features on the silicon wafer need to be developed before attempting to bond in this manner. The exposed bonding method needs to be better tuned to insure that the surfaces are properly bonded together, possibly applying more pressure for a longer period of time. Positive photoresist SC1827 is not suitable as a sacrificial layer, since SU-8 features did not adhere well to the layer that would also dissolve in SU-8 developer solution. Silicon dioxide could still be a possible way

to release the wafer, but testing this theory was not necessary without a proper way to bond the SU-8 layers.

The concept seemed like a feasible alternative to the partial exposure method, since this would not require the use of the UV filter. Bonding proved to be difficult, as did wafer release, but a release step is unnecessary without successful bond.

5.4 Chapter Summary

Neither the partial exposure method nor the inverted build method was successful in creating our final device as we had intended. We faced problems during the fabrication using both processes, resulting in loss of features and ultimate failure in building our platform.

For the partial exposure method, we encountered two major problems. First, the UV filter did not have the desired effect on the SU-8 that we hoped it would. We did not achieve different levels of SU-8 height with increasing exposure energies, but instead, we were either overexposed or underexposed. Second, we continued to have issues with delamination of the SU-8 from the glass and between layers. Although the delamination between layers can be attributed to the improper use of the UV filter, our attempts at surface modification did not improve adhesion of SU-8 to glass.

For the inverted build method, we could not properly transfer the pattern from a silicon wafer to a glass slide. The first main issue was our inability to bond the SU-8 layers together from the two separate substrates. During the exposed bonding process, the layers did not adhere well to each other and would fall apart during development. The unexposed bonding method resulted in accidental exposure of the patterns on the wafer during the backside exposure. The second concern for this inverted build method was the release

mechanism. Although theoretically the sacrificial layers can be removed to release the wafer, having positive photoresist SC1827 or silicon dioxide on the silicon wafer sometimes hindered proper patterning of the fine features in SU-8. Tests for release were also rendered unnecessary when neither bonding processes were successful in transferring the two-layer pattern from the wafer to the glass substrate.

Through many attempts to fabricate this platform, we have learned that the photolithography process can be very unpredictable, and each step must be done properly to achieve desired results. Even though we had modified some experiments to fit our requirements, we were ultimately unable to fabricate an optically clear SU-8 device on a glass substrate.

CHAPTER 6

Future Work

6.1 PDMS Nanochannels

Since fabrication of the device using SU-8 on glass has not been successful, we look for other options to create these platforms. Working with collaborators Cong Wu and Professor Wen J. Li from the Department of Mechanical and Biomedical Engineering from City University of Hong Kong, we move toward a future direction to form enclosed channels in a PDMS substrate.

A common method for creating PDMS devices utilizes a mastermold, fabricated using SU-8 on a silicon wafer from standard photolithography techniques. However, the minimum height of SU-8 exceeds desired dimensions for these channels. Using a nano-indenter, a needle scratches the surface of a hard plastic PMMA to create channels. PDMS is then molded on the hard plastic to create a negative master mold, and duplicates of the original PMMA channels can be molded again in PDMS.

Using atomic force microscopy (AFM), surface profiles can be measured to show a 100μm long channel with approximately 250nm depth and 1.5μm width. Figure 6.1 below shows AFM-scanned images of the nanochannel pattern in PMMA and the molded nanochannel pattern in PDMS to depict the surface profiles. These images are provided courtesy of our collaborators. Figure 6.2 shows the actual PDMS samples at 1x and 20x magnification taken using an optical upright microscope.

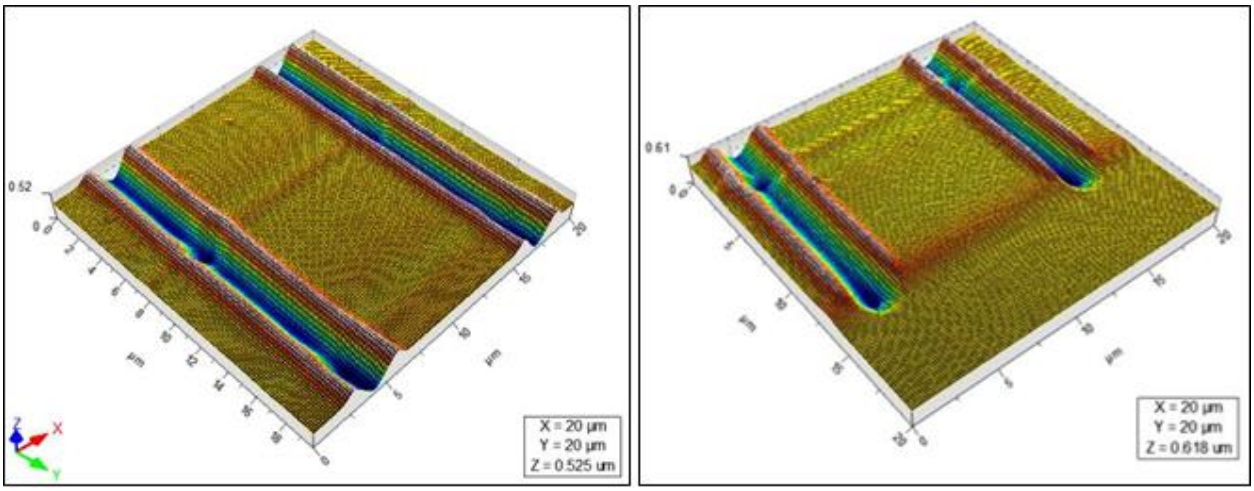

Figure 6.1: AFM-Scanned Surface Profiles [27]**.** (Left) The surface profile of the PMMA plastic shows approximately 250nm depth and 1.5µm width for each channel. (Right). The molded channels in PDMS show similar dimensions to the original PMMA channels.

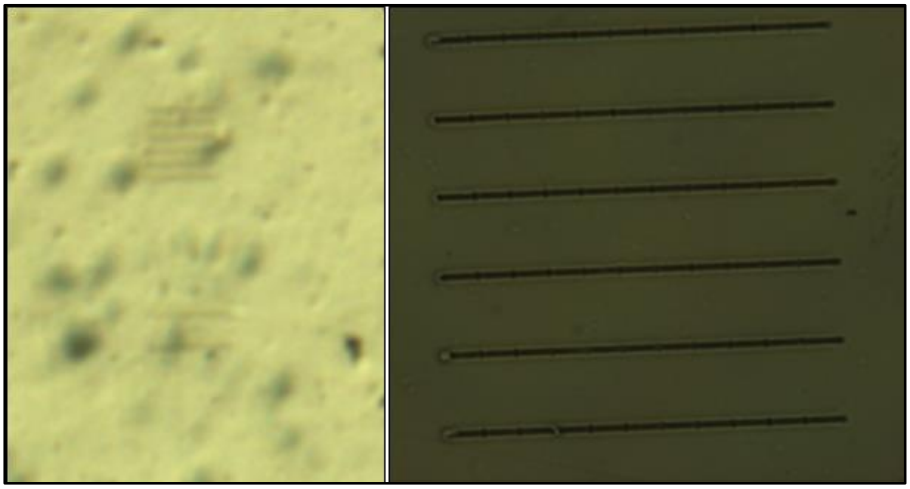

Figure 6.2: PDMS Nanochannels. (Left) 100µm nanochannels on a PDMS substrate are barely visible at 1x. (Right) A magnification of 20x allows for better visualization.

Although visible at 20x magnification, Scanning Electron Microscopy (SEM) is utilized to obtain a better image at higher levels of magnification. For SEM, a beam of electrons scans the surface of the substrate to produce images. Electrons interact with the atoms in the sample, so the surface of interest must be electrically conductive and must be electrically grounded as to not build up charge from the electron beam.

Since the features are on a PDMS sample, the substrate needs to be coated in a thin layer of metal to make the surface electrically conductive. Using an e-beam evaporator, a thin 100 Angstrom layer of chrome is deposited onto the surface of the PDMS containing the nanochannel features. Shown below in Figure 6.3 are images of the nanochannels at 1100x and 2000x magnification using SEM.

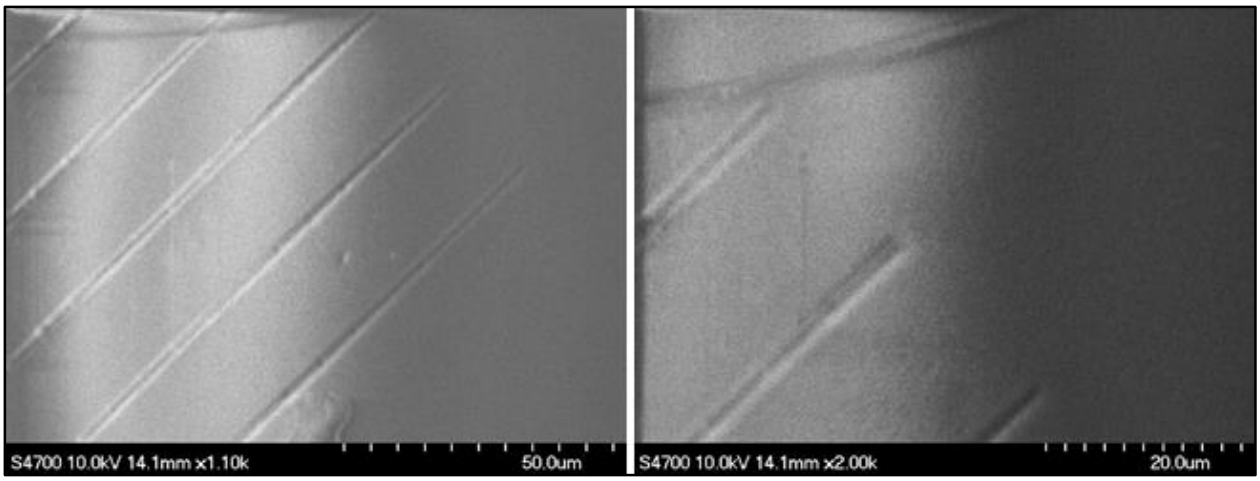

Figure 6.3: SEM Images of PDMS Nanochannels. (Left) Nanochannels are visualized using SEM at 1100x magnification. (Right) Images are taken at 2000x magnification to visualize the width of the nanochannel.

Due to the shallow nature of the channels, it is difficult to properly focus the electron beam on the appropriate area and zoom in to locate the channels. The PDMS sample must be carefully marked to know the exact location of the channels.

Next, we wanted to cut across the channels to obtain a cross-sectional view. Using a razor blade and upright microscope, we were able to cut across the channel, despite many issues with proper positioning. Since the channels are 100μm long, approximately the width of a strand of hair, it is difficult to cut accurately within a small window of space. The width of the razor blade may also be wider than the channels, although able to achieve a relatively

clean cut. Figure 6.4 shows many missed cuts on one sample and a successful cut on another sample at 5x magnification.

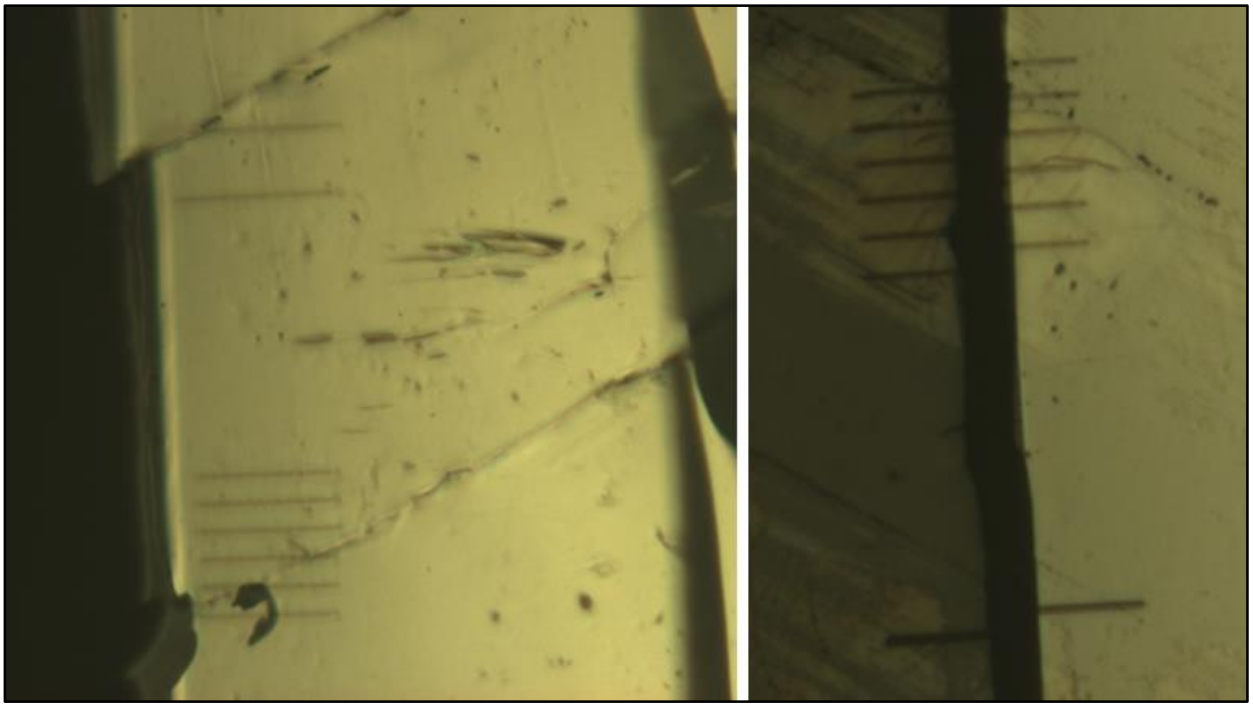

Figure 6.4: Cut Attempts on PDMS Nanochannels. (Left) Multiple missed cuts on the PDMS sample to the left and to the right of the channel area, which left the 100μm channels intact. (Right) Successful cut across the channels, which would allow for proper visualization of the cross-sectional area.

The sample must undergo another e-beam metallization process to coat the newly exposed cross-sectional area for SEM imaging. However, we were not able to acquire clean images to measure the cross-sectional area. The shallow depth and possibly slanted cut of the razor blade left a slight ledge near the nanochannel area, which interfered with our ability to obtain measurements. Figure 6.5 shows the SEM image of the cut nanochannel sample tilted at a 45° angle at 900x magnification and 2000x magnification.

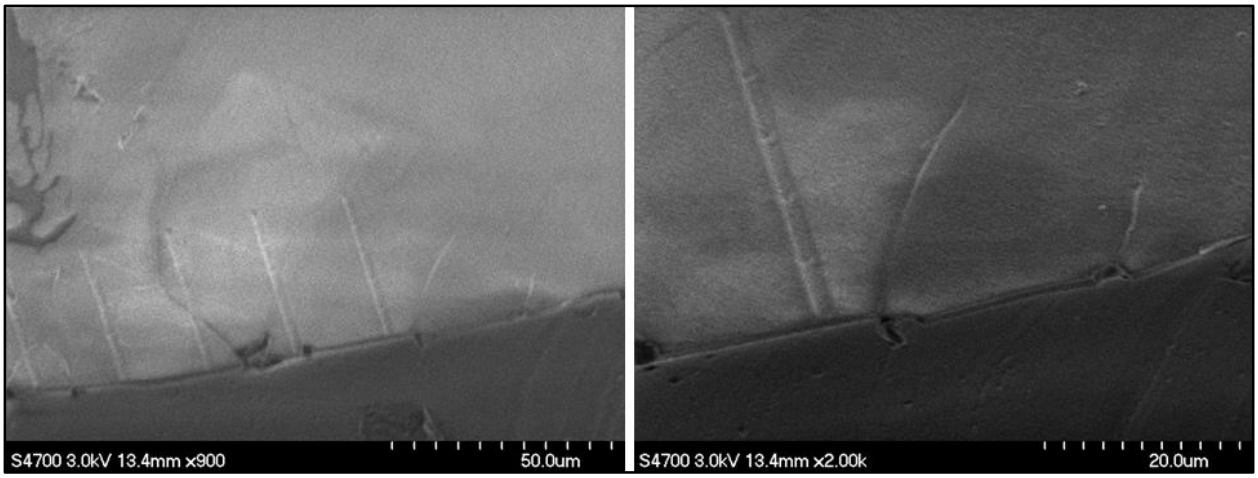

Figure 6.5: SEM Images of Cut PDMS Nanochannels. (Left) At 900x magnification, a ledge is visible near the opening of the channel. (Right). The edge of nanochannel base is difficult to separate from the ledge, even at 2000x magnification.

We were able to acquire SEM images of the nanochannels and cut across them, but the actual dimensions of the nanochannels were unable to be measured. There was much difficulty involved in locating the channels using SEM due to the shallow depth of the nanofeatures.

6.2 Enclosed PDMS Nanochannels

The next step would be to enclose the nanochannels with another layer of PDMS. This secondary piece of PDMS would contain separate larger area chambers to contain cells, connected only by the nanochannels in the original PDMS sample. The two pieces of PDMS are plasma bonded together to create an irreversible seal. Figure 6.6 below shows a schematic of the formation of the enclosed nanochannels, while Figure 6.7 shows the actual PDMS sample.

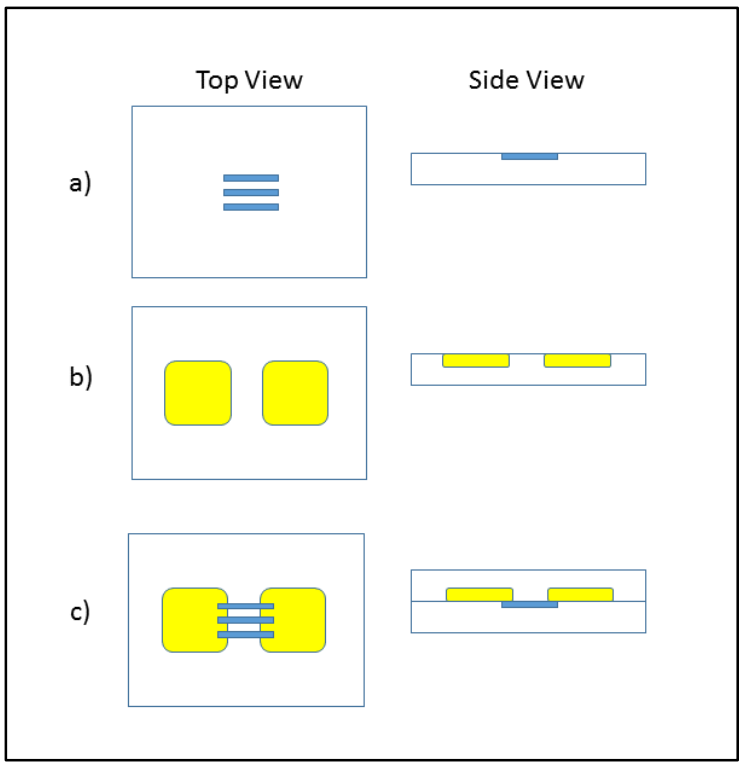

Figure 6.6: Enclosed PDMS Nanochannels Process Flow. Schematic diagram of enclosed nanochannels formed from two pieces of PDMS. a) One piece of PDMS contains the nanochannels molded from a nano-indented surface. b) Another piece of PDMS is molded to create chambers created using standard photolithography. c) The surfaces are plasma bonded together to connect the separate chambers and enclose the nanochannel.

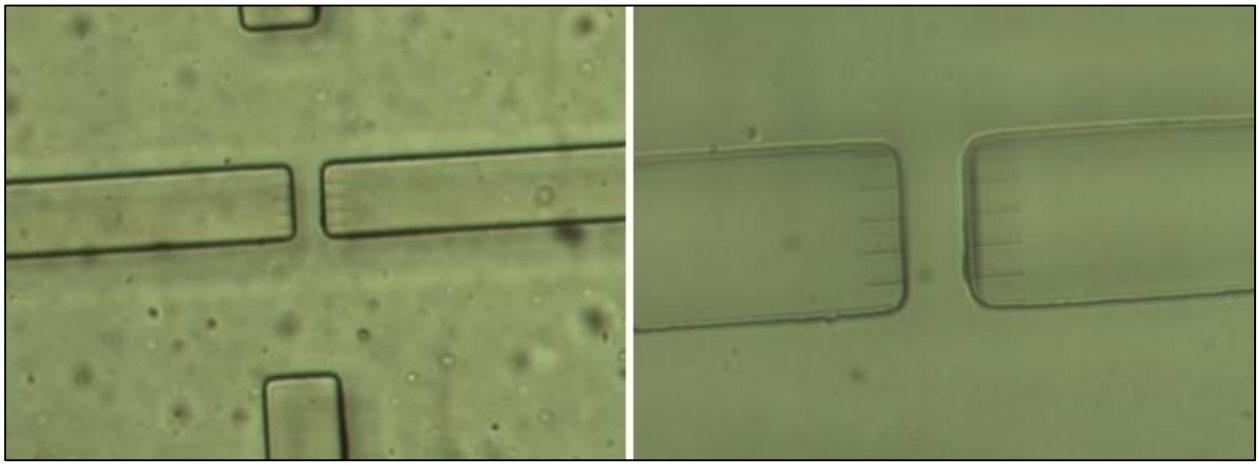

Figure 6.7: Enclosed PDMS Nanochannels. (Left) Images taken at 2x, with four microchambers visible. (Right) A 5x magnification image shows the two microchambers connected by the nanochannels.

Like the previous open nanochannels, we want to cut across the sample to obtain a cross-sectional view. However, there is a smaller working distance of approximately 50μm in which to try to cut, given the same original 100μm nanochannels. It is not possible to cut these channels with the same razor blade and upright microscope setup due to the smaller window of space and error rate.

We explore the use of a vibrating microtome, or vibratome, to shave pieces of the PDMS. Normally used to handle delicate biological samples, a vibratome can be programmed to cut a sample into 5μm slices. However, a thickness of approximately 50μm is more realistic and visible while the sample is actually being sliced. With help from the Glabe Lab at UCI, the vibratome setup is shown below in Figure 6.8.

Figure 6.8: Vibratome Setup. (Left) The vibratome features dials to control the speed of the blade and section thickness, and a multi-well plate is used to store sample slices. (Right) Through the 2x magnification lens, we can see the blade as it approaches the sample, which has been glued to a plastic substrate to maintain proper positioning. (Facility: Glabe Lab at UCI.)

The PDMS sample is glued onto a plastic substrate so that it can be placed into the stand of the vibratome. The blade slowly moves forward to cut through the sample, producing slices depending on the height set by the user. The delicate slices are picked up using a paint brush and stored in separate chambers in the multi-well plate. Using an upright microscope, we can image the 50um slices to visualize the cross-sectional area. Given the layout of the PDMS sample with enclosed nanochannels, slices around the nanochannels should reveal cross-sections of the microchambers, as shown below in Figure 6.9.

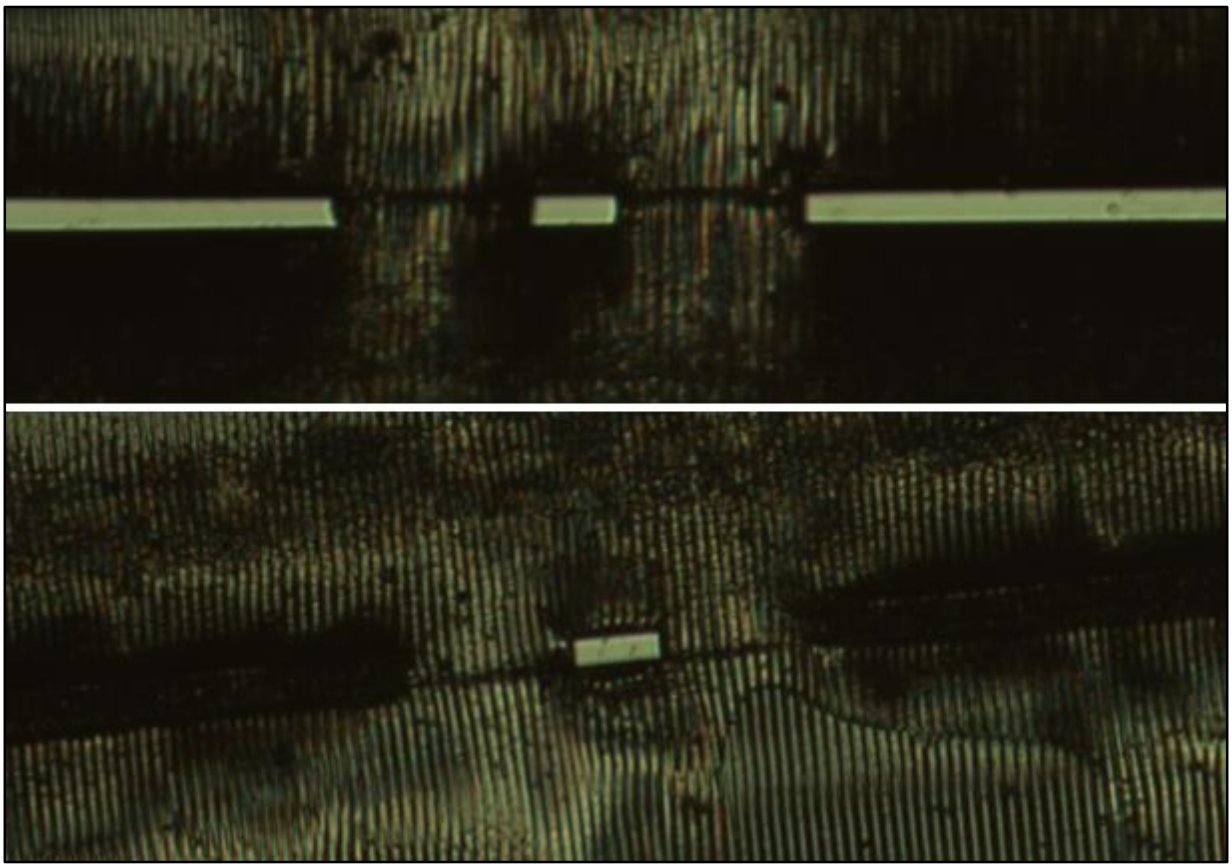

Figure 6.9: Cross-Sectional PDMS Slices. (Top) A slice of PDMS features the center microchamber, as well as two open microchambers on the side. (Bottom) The last slice shaved from the sample shows partially cut microchambers on the side.

The last slice shows that the sample has been shaved into the 50um window of space that contains only the nanochannels. As seen below in Figure 6.10 in a top view of the PDMS

sample, one microchamber connected by the nanochannels has been removed, and the cross-sectional face should only contain the nanochannels.

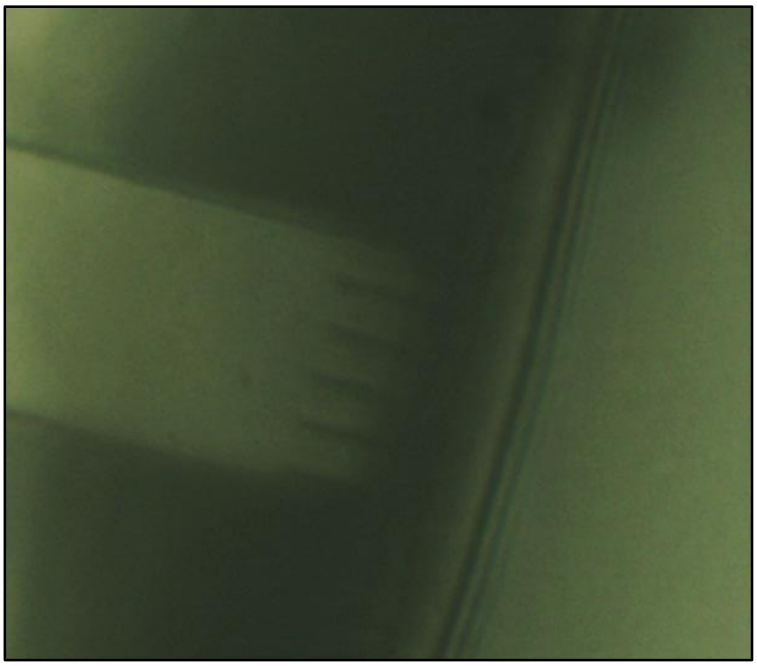

Figure 6.10: Top view of Enclosed Nanochannels. After consecutive shavings of the sample, the original sample is now cut down in the intermediate area between the microchambers shown in Figure 6.6, so the cross-section should reveal only nanochannel openings.

The cross-sectional face of the sample is then coated with 100A of chrome using an e-beam evaporator and imaged using SEM. The microchambers on the side are easily visualized, so the nanochannels should be located halfway in between these features. Also, the microchamber below the nanochannels is somewhat visible, as shown in Figure 6.11.

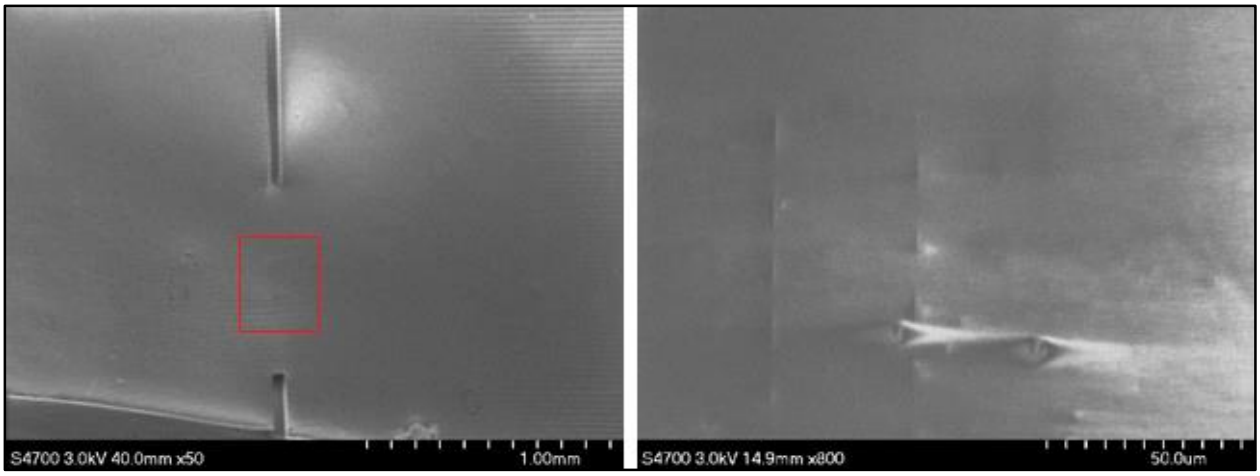

Figure 6.11: SEM Images of Enclosed Nanochannels. (Left) Microchambers are visible at 50x magnification, so the nanochannels must be in between these features next to the microchamber located below it, as marked by the rectangle. (Right). An 800x magnification of the center microchamber below the surface, with possible nanochannel openings.

The microchambers help to locate the positioning of the nanochannels, but the images in Figure 6.11 are inconclusive. Although it appears that there might be some bright spots at 800x magnification that could possibly be the openings of the nanochannels, it is not clear if those are actual features or shadow artifacts from the SEM. With higher magnification, we lose visibility of the microchambers and any point of reference. Also, charge begins to build up on the surface from the electron beam used in SEM, washing out the contrast and visibility in the images.

Although it is difficult to visually confirm the geometry and physical boundaries of the channels, our collaborator has been able to perform flow tests in the nanochannel. The flow experiments confirm the connectivity of the two microchambers through the nanochannel without any leakage.

This method of creating enclosed nanochannels is promising to build our ultimate platform. Future experiments would include optimizing the dimensions of the microchambers to create suitable areas for cells and proper inlets and outlets for cell seeding and culture.

REFERENCES

[1] S. Maeda and T. Tsukihara, "Structure of the gap junction channel and its implications for its biological functions," *Cell. Mol. Life Sci.*, vol. 68, no. 7, pp. 1115–1129, 2011.

[2] S. K. Sia and G. M. Whitesides, "Microfluidic devices fabricated in poly(dimethylsiloxane) for biological studies," *Electrophoresis*, vol. 24, no. 21, pp. 3563–3576, 2003.

[3] M. B. Byrne, L. Trump, A. V. Desai, L. B. Schook, H. R. Gaskins, and P. J. a. Kenis, "Microfluidic platform for the study of intercellular communication via soluble factor-cell and cell-cell paracrine signaling," *Biomicrofluidics*, vol. 8, no. 4, p. 044104, 2014.

[4] N. V Menon, Y. J. Chuah, B. Cao, M. Lim, and Y. Kang, "A microfluidic co-culture system to monitor tumor-stromal interactions on a chip.," *Biomicrofluidics*, vol. 8, no. 6, p. 064118, 2014.

[5] P. J. Lee, P. J. Hung, R. Shaw, L. Jan, and L. P. Lee, "Microfluidic application-specific integrated device for monitoring direct cell-cell communication via gap junctions between individual cell pairs," *Appl. Phys. Lett.*, vol. 86, no. 22, pp. 1–3, 2005.

[6] A. Rustom, R. Saffrich, I. Markovic, P. Walther, and H.-H. Gerdes, "Nanotubular highways for intercellular organelle transport.," *Science*, vol. 303, no. 5660, pp. 1007–1010, 2004.

[7] S. Abounit and C. Zurzolo, "Wiring through tunneling nanotubes - from electrical signals to organelle transfer," *J. Cell Sci.*, vol. 125, no. 5, pp. 1089–1098, 2012.

[8] G. P. Dubey and S. Ben-Yehuda, "Intercellular nanotubes mediate bacterial communication," *Cell*, vol. 144, no. 4, pp. 590–600, 2011.

[9] Dow Chemical Company, "Microposit S1800 G2 Series Photoresists," *Data Sheet*, no. October. pp. 1–6, 2006.

[10] UCI Integrated Nanosystems Research Facility, "Lift-Off Procedure," no. November. p. 2007, 2007.

[11] M. Shaw, D. Nawrocki, R. Hurditch, D. Johnson, M. Corp, and N. Ma, "Improving the Process Capability of SU-8 2." .

[12] Microchem, "Negative Tone Photoresist Formulations 2– 25." pp. 1–4, 2002.

[13] Microchem, “SU-8 2000 Permanent Epoxy Negative Photoresist Processing Guidelines for: SU-8 2000.5, SU-8 2002, SU-8 2005, SU-8 207, SU-8 2010 and SU-8 2015,” *Product Datasheet*. 2000.

[14] Microchem, “SU-8 2000 Permanent Epoxy Negative Photoresist Processing Guidelines For: SU-8 2025, SU-8 2035, SU-8 2050 and SU-8 2075,” *Product Datasheet*. 2000.

[15] Microchem, “SU-8 3000 Permanent Epoxy,” *Product Datasheet*, vol. 20. 2000.

[16] L. J. Guerin, M. Bossel, M. Demierre, S. Calmes, and P. Renaud, “Simple and low cost fabrication of embedded micro-channels by using a new thick-film photoplastic,” *Proc. Int. Solid State Sensors Actuators Conf. (Transducers ’97)*, vol. 2, pp. 1419–1422, 1997.

[17] F. J. Blanco, M. Agirregabiria, J. Garcia, J. Berganzo, M. Tijero, M. T. Arroyo, J. M. Ruano, I. Aramburu, and K. Mayora, “Novel three-dimensional embedded SU-8 microchannels fabricated using a low temperature full wafer adhesive bonding,” *J. Micromechanics Microengineering*, vol. 14, no. 7, pp. 1047–1056, 2004.

[18] S. Tuomikoski and S. Franssila, “Free-standing SU-8 microfluidic chips by adhesive bonding and release etching,” *Sensors Actuators, A Phys.*, vol. 120, no. 2, pp. 408–415, 2005.

[19] F. Ceyssens and R. Puers, “Creating multi-layered structures with freestanding parts in SU-8,” *J. Micromechanics Microengineering*, vol. 16, no. 6, pp. S19–S23, 2006.

[20] UCI Integrated Nanosystems Research Facility, “HF (2 %) DIP.” pp. 1–3.

[21] M. Bachman, “RCA-1 Silicon Wafer Cleaning,” *INRF application note, UCI Integrated Nanosystems Research Facility*. pp. 1–3, 1999.

[22] P. Mak, “Piranha Clean Procedure,” pp. 1–3, 2010.

[23] Microchem, “SU-8 Permanent Photoresists.” 2000.

[24] Integrated Micro Materials, “Photoresist Adhesion and HMDS (hexamethyldisilazane) Processing,” *2013*. [Online]. Available: http://www.imicromaterials.com/index.php/technical/HMDS.

[25] Yield Engineering Systems, “YES HMDS Vapor Prime Process Application Note.” pp. 1–6.

[26] UCI Integrated Nanosystems Research Facility, “Buffered Oxide Etch.” pp. 1–3.